

DESIGN AND FABRICATION OF A  
SKIN STRINGER DISCRETE TUBE  
ACTIVELY COOLED STRUCTURAL PANEL\*

Frank M. Anthony  
Bell Aerospace Textron  
Buffalo, N.Y.

INTRODUCTION

A number of structural concepts have been proposed and investigated for hypersonic aircraft. When such aircraft are powered by hydrogen fueled advanced airbreathing engines the heat capacity of the fuel exceeds engine cooling requirements. The excess provides an attractive heat sink for actively cooled airframe structure. Analytical studies of a hypersonic transport indicated a potentially large weight reduction if liquid cooled aluminum alloy construction could be used. Consequently, the Langley Research Center of NASA initiated several programs (Ref. 1) to investigate the design optimization and practical implementation of actively cooled structural panel concepts.

\*This paper reviews the work performed on one particular concept by Bell Aerospace Textron under Contract NAS 1-12806. The design of the test panel resulting from this effort was derived from the optimized design of a full sized panel. The test panel will be delivered soon for experimental evaluation at the Langley Research Center.

SKIN STRINGER DISCRETE TUBE  
ACTIVELY COOLED STRUCTURAL PANEL

(Figure 1)

The desired actively cooled structural panel consisted of the cooled skin and a substructure whose functions are indicated. Conventional materials were used throughout. The primary load carrying components were fabricated from 2024-T3 aluminum alloy. The 3003-H14 coolant passage tubing was chosen because of its excellent corrosion resistance, workability needed to obtain the desired cross sectional shape, and strength. The Epon 951 adhesive was selected for its excellent structural properties and is the thinnest of available films, 0.064 mm (0.0025 in.). The Eccobond 58C silver filled epoxy was chosen because of its high thermal conductivity, and the alumina filled Epon 828 was chosen for structural and expansion characteristics.

# SKIN STRINGER DISCRETE TUBE ACTIVELY COOLED STRUCTURAL PANEL CONTRACT NAS 1-12806

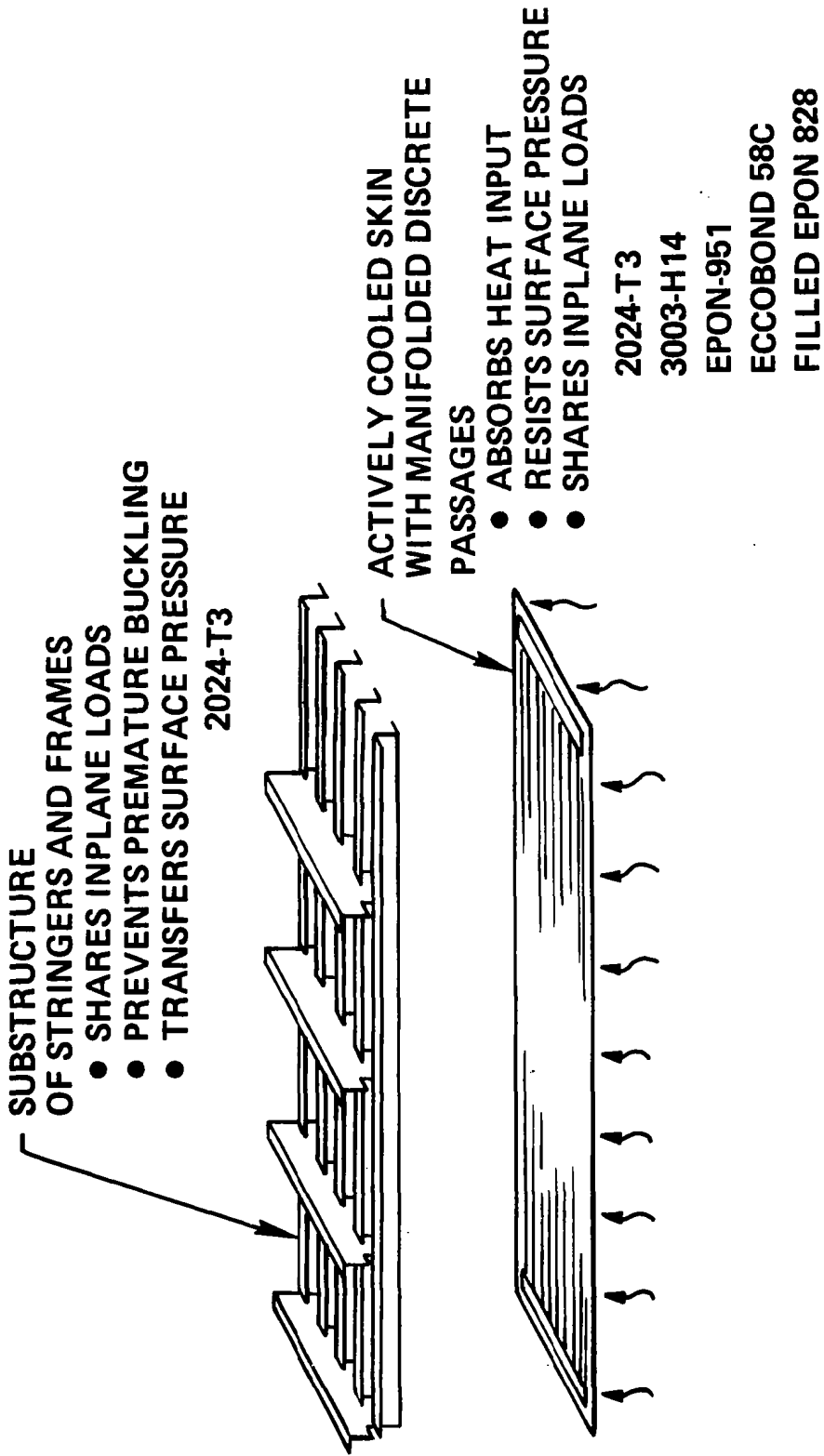


Figure 1

## REDUNDANT COUNTERFLOW COOLANT CIRCUITS ARE USED

(Figure 2)

The preceding figure presented an overview of the cooled structural panel approach. This figure provides details of the coolant circuit within the skin. Two adjacent tubes of a quarter elliptical cross section form the passages through which the coolant flows in opposite directions. The two independent circuits provide redundancy. Coolant is introduced to a multiplicity of parallel paths in each circuit through manifolds at the outer edge of the panel and transverse to the coolant passages. The manifold contains two parallel coolant plenums, the supply for one coolant circuit and the return from the other. Holes through the wall of the plenums connect them to the individual coolant passages.

Concern for damage tolerance led to the investigation of crack arrestors which could be incorporated in the beads which contained the coolant passage tubing. These crack arrestors were evaluated as part of an inhouse program. Their incorporation into a panel of relatively large size posed fabrication difficulties. Therefore, they were excluded from the final test panel even though they had been used for the fatigue test specimens that will be discussed later.

# REDUNDANT COUNTERFLOW COOLANT CIRCUITS ARE USED

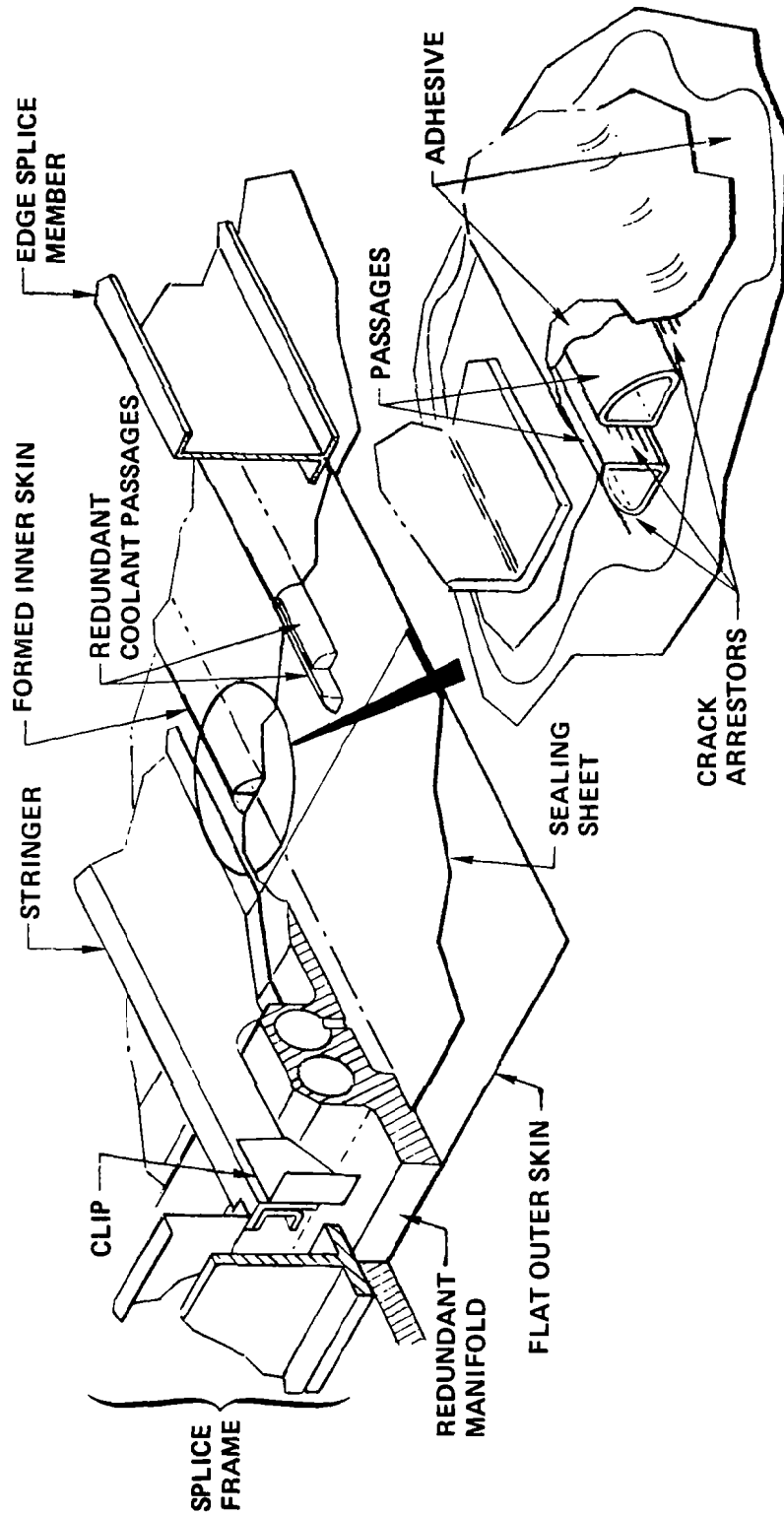


Figure 2

## DESIGN REQUIREMENTS

(Figure 3)

The requirements listed here were considered representative of the lower surface of a hypersonic transport. Local environmental conditions, factors of safety and life related considerations are included. The primary environmental conditions were defined by NASA. Supplementary requirements were introduced by Bell to further specify detailed requirements.

# DESIGN REQUIREMENTS

## NASA

HEAT FLUX 136 kW/m<sup>2</sup> (12 BTU/ft<sup>2</sup>sec)  
INPLANE LOADING ± 210 kN/m (±1200 lb/in.)  
PRESSURE LOADING ± 6.89 kPa (± 1.0 psi)  
DESIGN LIFE 5000 CYCLES  
ALUMINUM ALLOY MATERIALS COMPATIBLE WITH COOLANT  
LENGTH AND WIDTH 6.1 x 0.61 m (20 x 2 ft)  
FRAME SPACING 0.61 m (2 ft)  
OUTLET PRESSURE 345 kPa (50 psi)

## BELL

LIFE SCATTER FACTOR 4.0  
FACTORS OF SAFETY LOADS 1.0 LIMIT/1.5 ULTIMATE  
TEMPERATURE 1.0 LIMIT/1.0 ULTIMATE  
PRESSURE ONLY 1.5 PROOF/2.0 ULTIMATE  
STRENGTH ALLOWABLES BASED ON 10,000 HOURS OF EXPOSURE  
REDUNDANT COOLANT CIRCUITS

Figure 3

### MANY PARAMETERS INFLUENCE PANEL OPTIMIZATION

(Figure 4)

Optimization of an actively cooled structural panel requires consideration of a large number of parameters which may be grouped into three broad categories, thermal, structural, and environmental. By investigating the relationships among the various parameters, it is possible to define the materials and geometric configuration which result in a cooled panel of minimum mass. For this particular project the environmental conditions were defined. In the general case thermal and structural consideration may modify the environmental aspects through changes to the aircraft or its flight path which minimize total system mass.



# MANY PARAMETERS INFLUENCE PANEL OPTIMIZATION

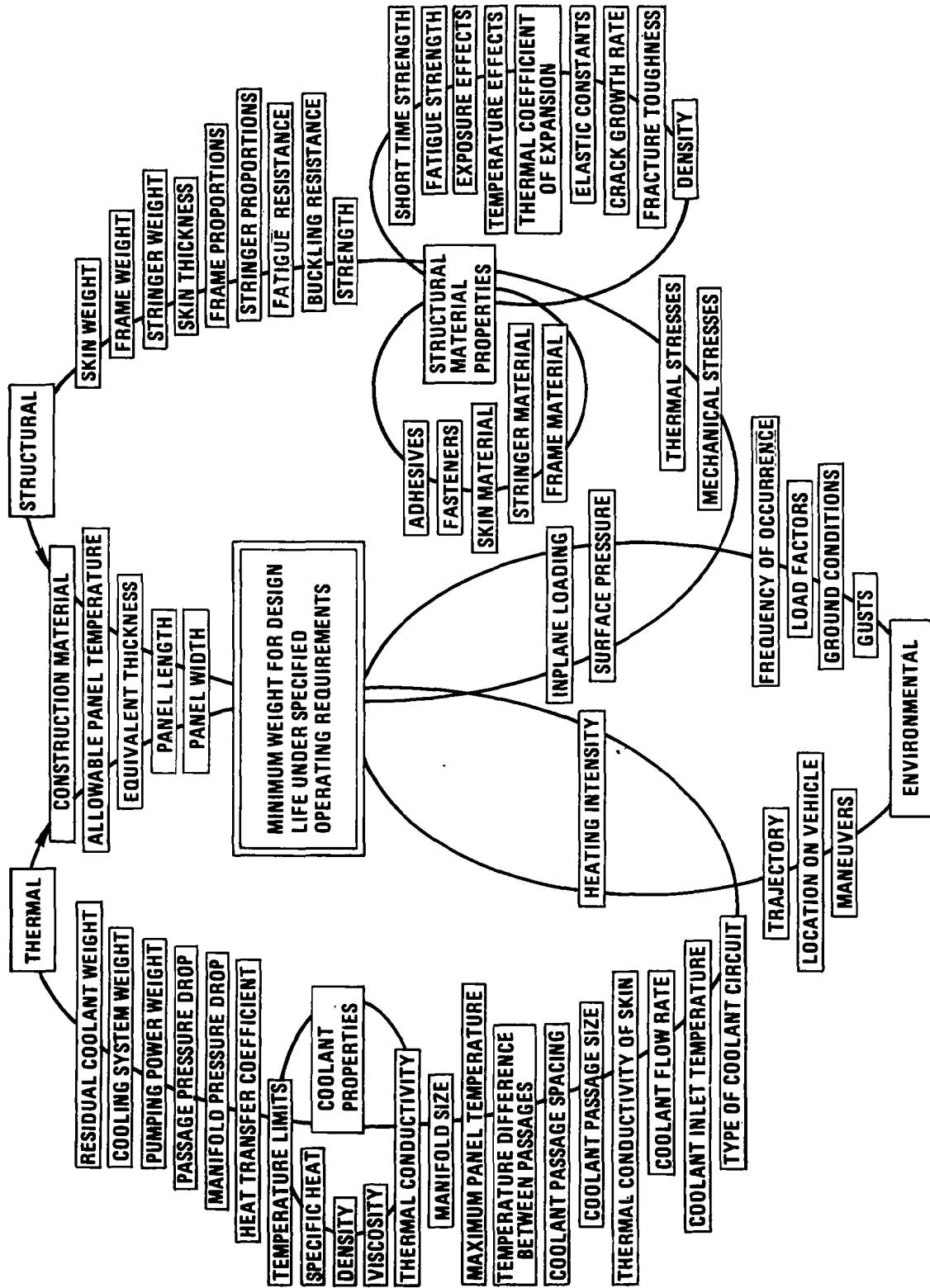


Figure 4

## REPETITION OF DESIGN PROCESS RELATES SKIN TEMPERATURE AND PANEL MASS

(Figure 5)

The iterative sequence for establishing optimum proportions for an actively cooled structural panel is illustrated here. The rectangular boxes define particular steps in the process. The oval boxes identify inputs. In essence a relationship is established between panel mass and maximum operating temperature. The panel mass reflects the material required to carry the structural loadings for the required number of cycles. This mass is distributed in such a way as to maximize the stability characteristics of the panel. The maximum temperature of the panel is controlled by the flow of coolant through passages within the panel so that the total panel weight includes contributions of coolant inventory and Auxiliary Power System mass.

Prior studies indicated that minimum mass is achieved when the equivalent skin thickness is minimized (ref. 2). Therefore, the analysis sequence begins by estimating this parameter from loading and material property data.

# REPETITION OF DESIGN PROCESS RELATES SKIN TEMPERATURE AND PANEL MASS

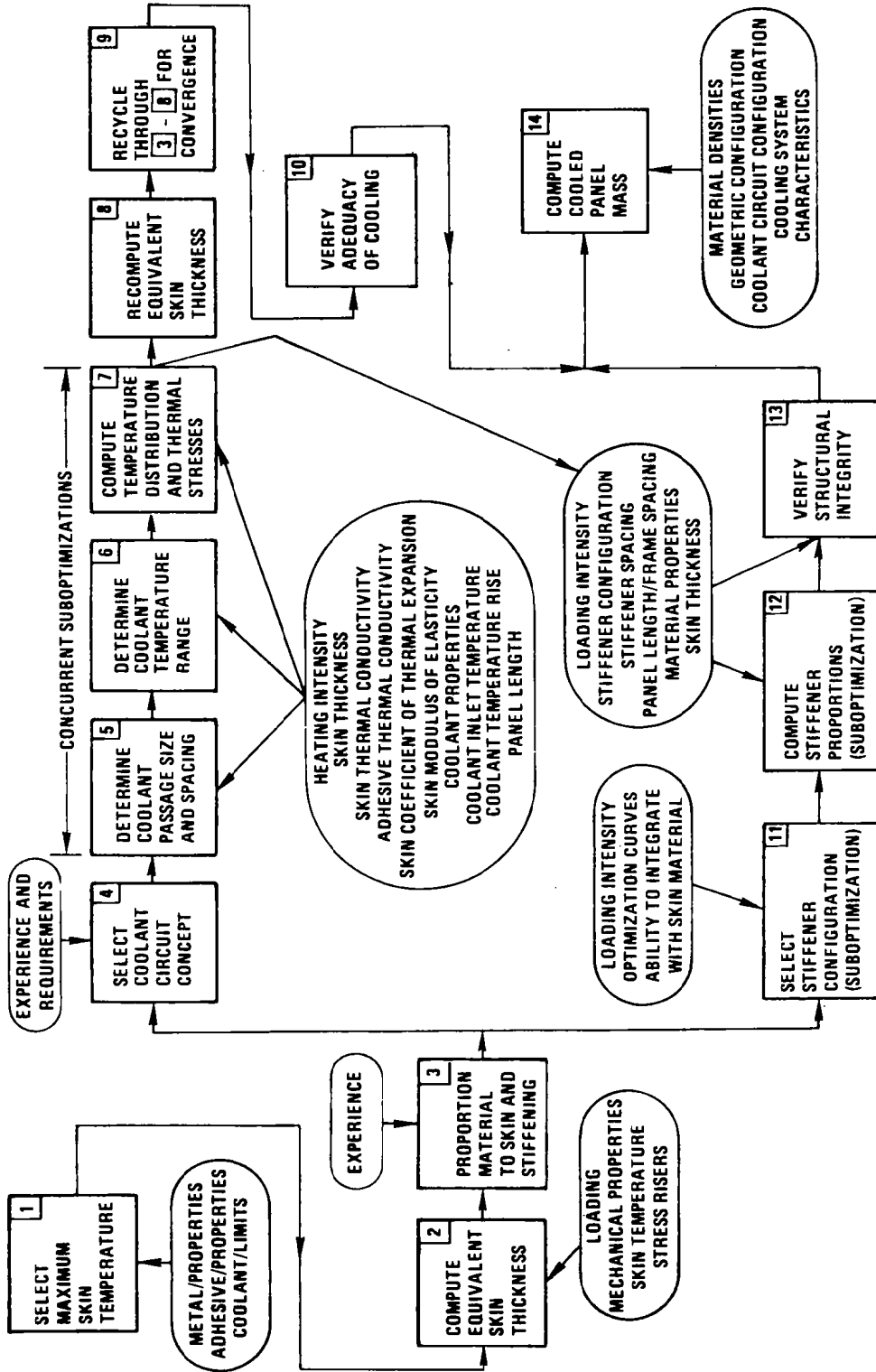


Figure 5

## COOLANT CIRCUIT CONCEPTS

(Figure 6)

Coolant can be distributed through the structural panel in a number of ways. For purposes of this design, the discrete coolant passage approach was selected because of its greater ease of integration with conventional construction techniques and the potential for minimum mass as indicated by prior studies (ref. 3).

Two versions of discrete passages were considered, the single passage/single pass approach and the counterflow/dual passage redundant arrangement. The latter was chosen because of its ability to provide a more uniform temperature distribution over the panel surface and the redundancy feature which would be desirable under emergency conditions.

# COOLANT CIRCUIT CONCEPTS

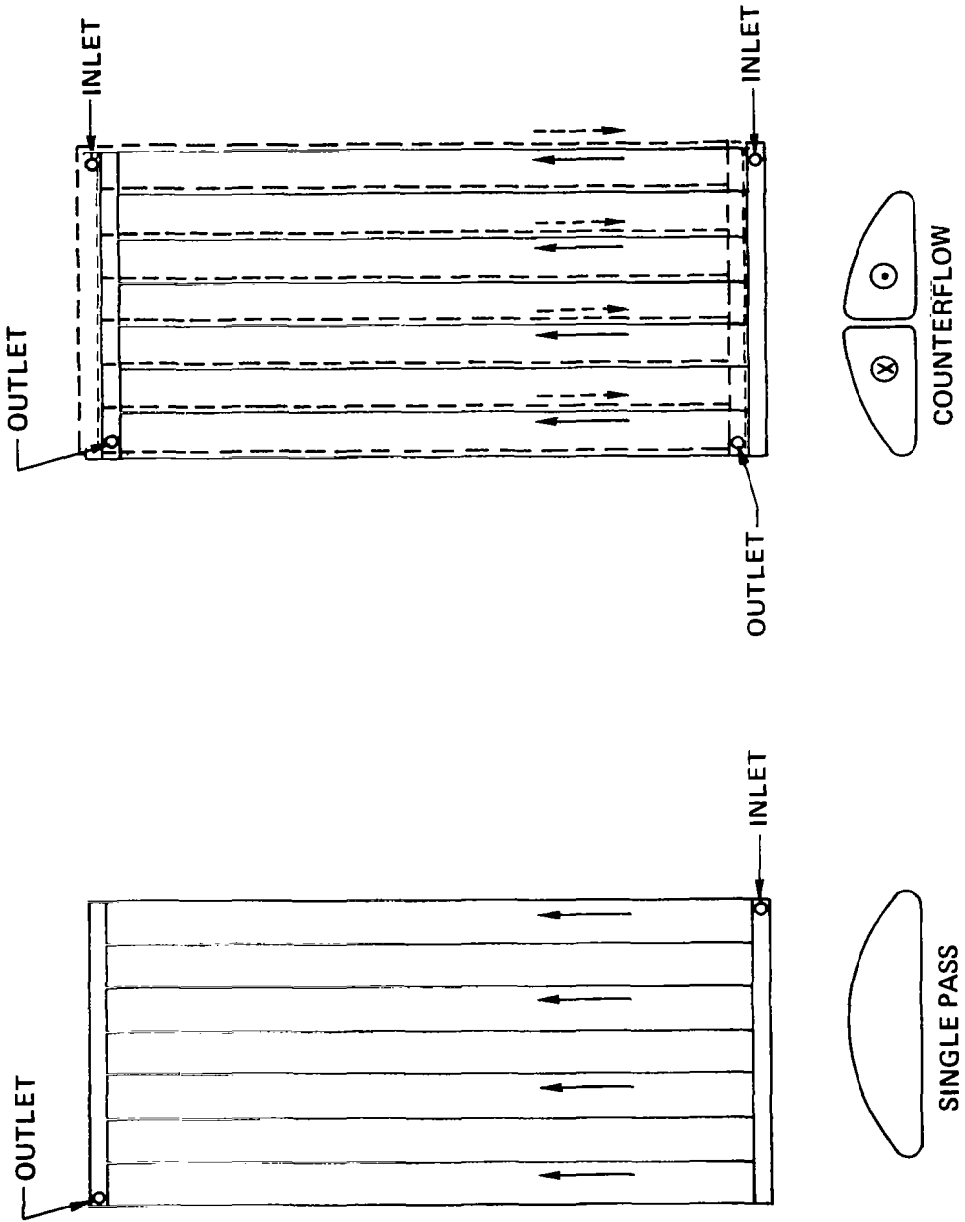


Figure 6

## COUNTERFLOW OF COOLANT MINIMIZES AXIAL TEMPERATURE DIFFERENCES

(Figure 7)

The temperature distributions in cooled panels which incorporate counterflow and single pass/single direction flow design concepts are quite different. In both cases the total coolant flow rate is the same so that the coolant temperature rise is the same. In the case of the single flow direction the very low inlet temperature results in a very low Reynolds number and heat transfer coefficient in the inlet region. The large temperature difference across the coolant film causes the maximum panel temperature to occur near the inlet rather than near the outlet as might be expected. When a counterflow arrangement is used there is very little temperature variation along the length of the panel in the direction of coolant flow. The low heat transfer coefficient near the inlet of one coolant passage is offset by the much higher heat transfer coefficient near the outlet of the adjacent coolant passage. There is relatively little difference in the temperature difference between the coolant passages. Directly over a passage the wall temperature is lower than half way between the discrete coolant passage locations.

# COUNTERFLOW OF COOLANT MINIMIZES AXIAL TEMPERATURE DIFFERENCES

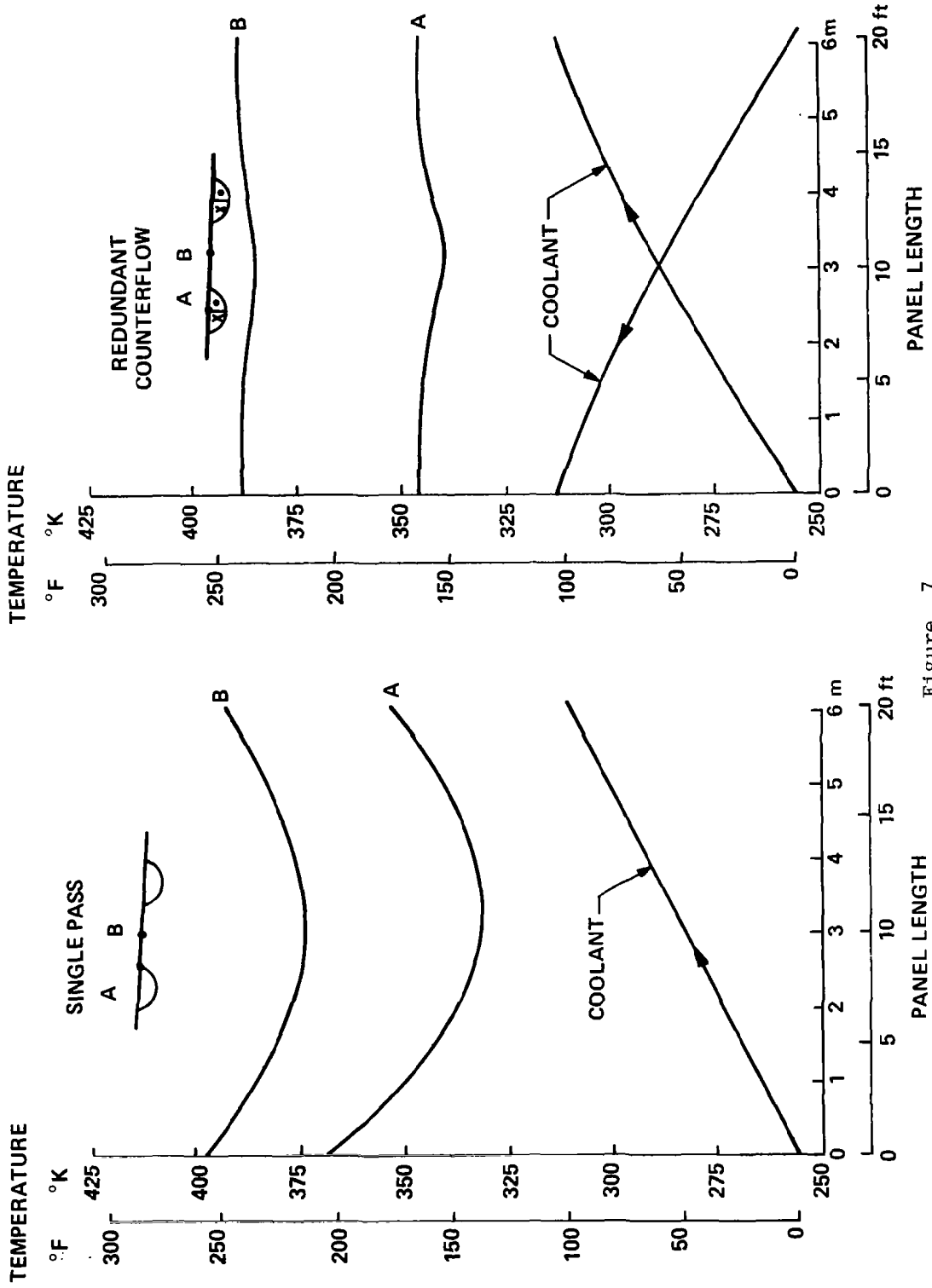


Figure 7

## MAXIMUM PANEL TEMPERATURE INCREASES WITH PASSAGE SPACING

(Figure 8)

To a first approximation, the spacing of the coolant passages is related to the temperature difference between passages by various physical parameters as indicated in the following equation:

$$(s - w) = \sqrt{\frac{8 t k \Delta T}{q}}$$

where  $s$  = passage spacing  
 $w$  = passage width  
 $t$  = skin thickness  
 $k$  = thermal conductivity  
 $\Delta T$  = skin temperature difference  
 $q$  = heat flux

When proper account is taken of the actual configurations and the thermal resistance of the adhesives, the relationship between maximum panel temperature and coolant passage spacing is as shown in this figure. The panel temperature is influenced by the inlet and outlet temperature of the coolant. These particular data were generated for an outer surface skin thickness of 0.8 mm (0.032 in), and inner skin thickness of 0.5 mm (0.02 in), a coolant passage wall thickness of 0.25 mm (0.01 in), and adhesive thickness of 0.064 mm (0.0025 in). Each of the data points represents an optimized combination of coolant passage and cooling system where the combined mass of the coolant inventory and the APS was minimized. Therefore, each combination represents a design with a different coolant passage width.



# MAXIMUM PANEL TEMPERATURE INCREASES WITH PASSAGE SPACING

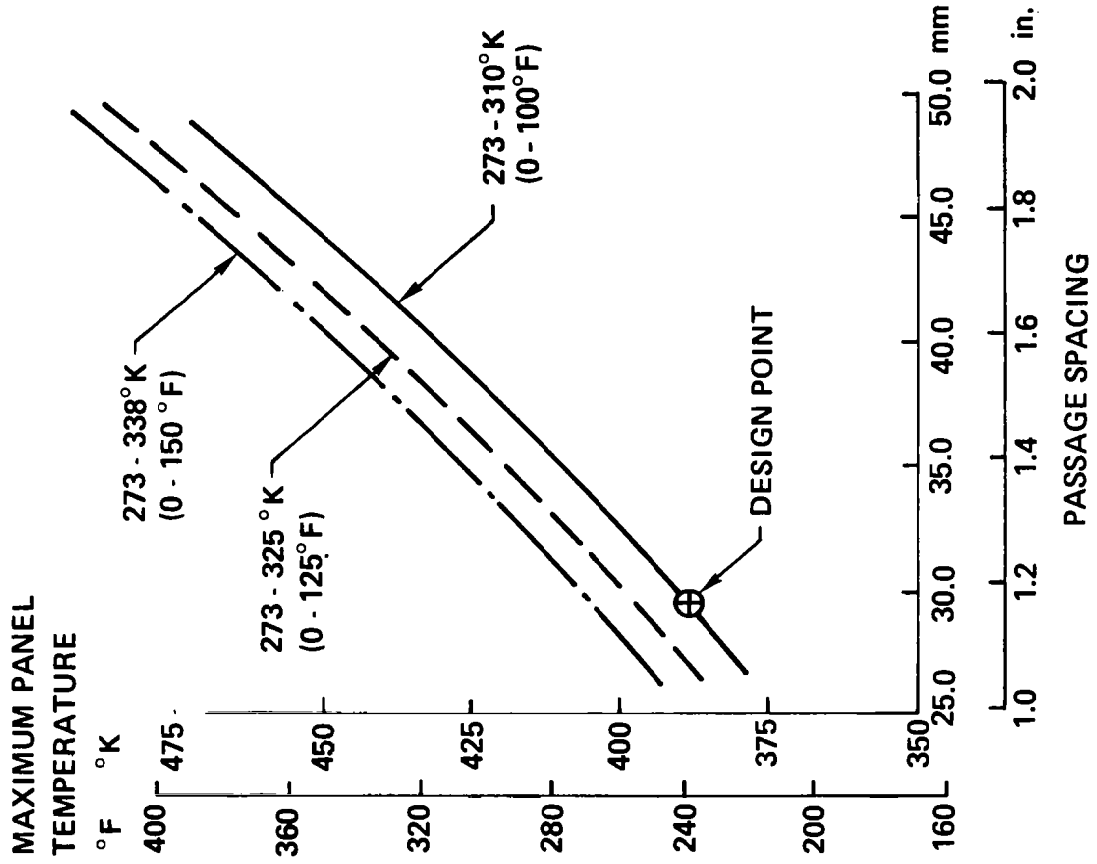


Figure 8

### OPTIMUM PASSAGE WIDTH INCREASES WITH PASSAGE SPACING

(Figure 9)

As the coolant passage spacing increases, the amount of coolant which must flow through a particular passage is increased. If the coolant passage cross section is maintained constant, this flow rate increase results in an increase in pressure drop. If the coolant passage cross section is allowed to increase as the flow rate increases, a minimum mass combination of coolant passage cross section (coolant inventory) and APS weight is achieved. The widths given on this plot are the optimums which result in this minimum combined mass. Over the range of coolant passage spacing examined, the coolant passage width is a relatively weak function of spacing. Passage width is more strongly a function of the coolant temperature rise.

The design point does not fall on any of the optimum lines because the coolant ducting was sized so that it could be formed from tubing of a standard diameter, 0.76 mm (0.25 in) for the selected configuration.

# OPTIMUM PASSAGE WIDTH INCREASES WITH PASSAGE SPACING

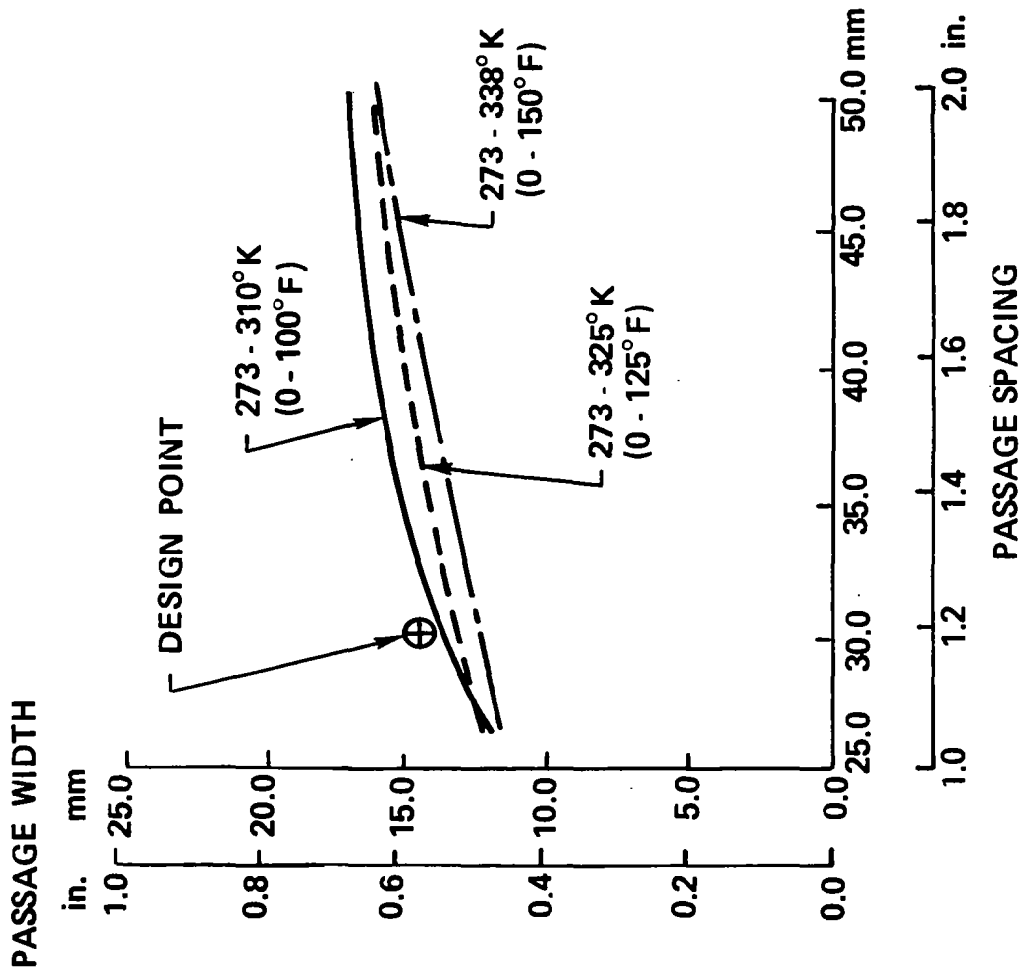


Figure 9

COOLANT TEMPERATURE HAS A GREATER  
INFLUENCE ON PRESSURE DROP  
THAN PASSAGE SPACING

(Figure 10)

The pressure drops shown on this plot are for a panel length of 6.1 m (20 ft). As the passage spacing increases, relatively more coolant flows through each passage, and as seen previously, the passage width increases. There is an increase in the coolant inventory within the passage. However, the larger cross-sectional area of the passage means a relative decrease in pressure drop for the same total flow through the panel. The net result is a decrease in pressure drop as the number of passages increases.

The pressure drop is more dependent on the coolant temperature level used for the design than on passage spacing. The temperature dependence of coolant viscosity is the dominant consideration.

# COOLANT TEMPERATURE HAS A GREATER INFLUENCE ON PRESSURE DROP THAN PASSAGE SPACING

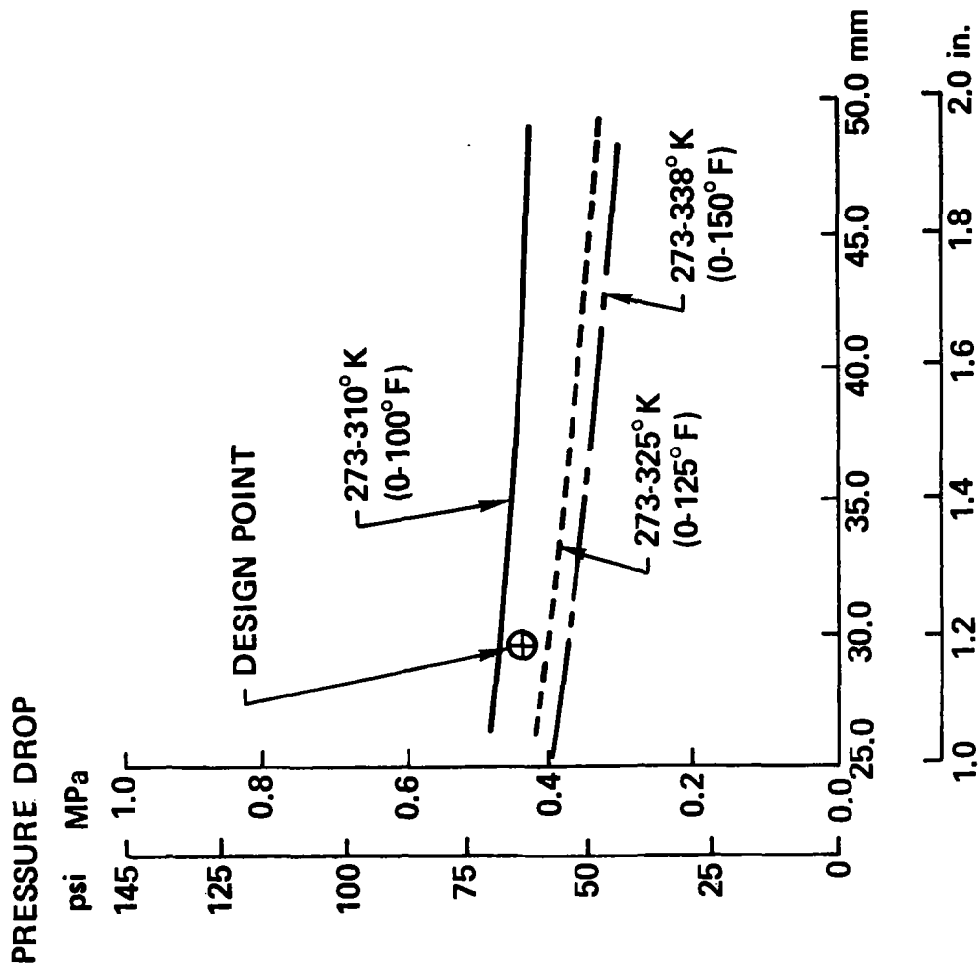


Figure 10

WEIGHT OF RESIDUAL COOLANT PLUS APS  
POWER IS INSENSITIVE TO PASSAGE SPACING

(Figure 11)

When the combined weight of the coolant inventory and APS mass is minimized the weight of these cooling system elements is a weak function of coolant passage spacing. The weight decreases slightly as coolant passage spacing increases. The coolant temperatures have a more significant influence on the mass of the cooling system elements because the coolant flow rate is directly proportional to the allowable coolant temperature rise through the panel and to the particular temperature levels as they affect coolant properties.

# WEIGHT OF RESIDUAL COOLANT PLUS APS POWER IS INSENSITIVE TO PASSAGE SPACING

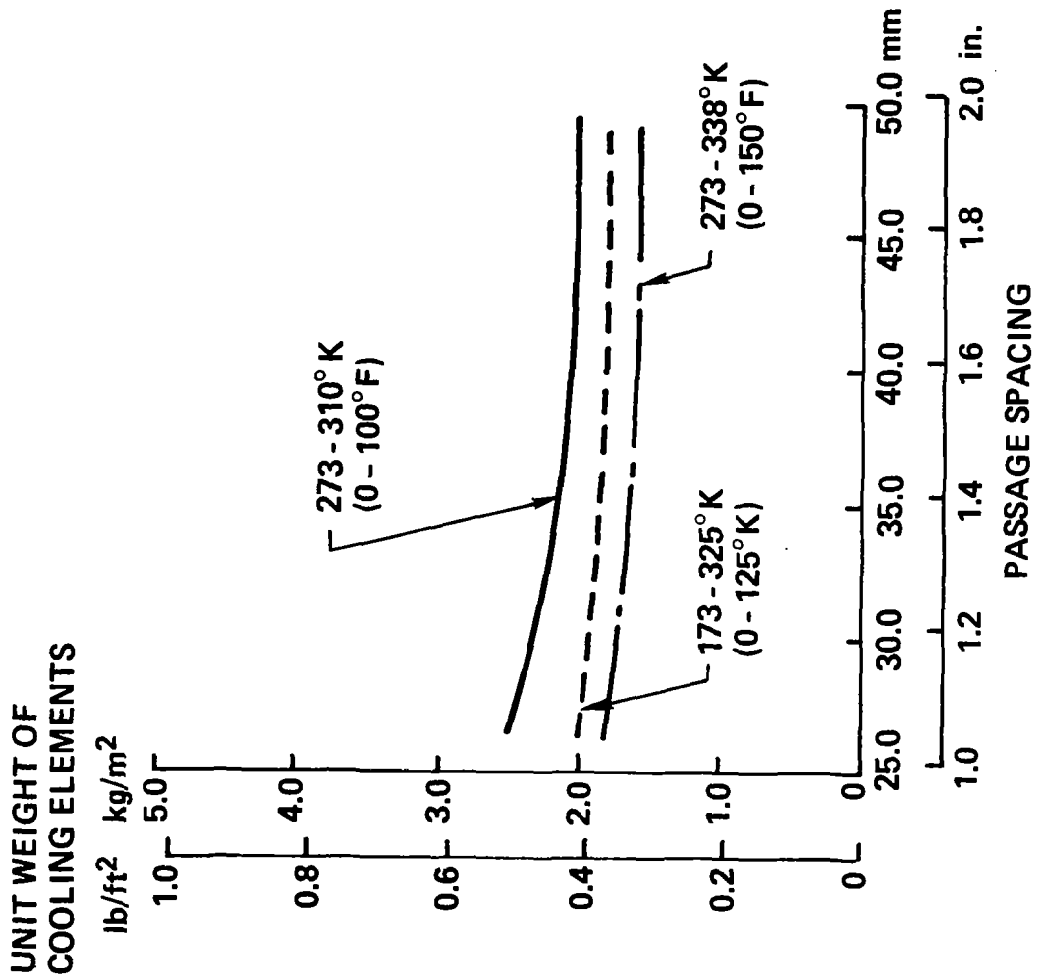


Figure 11

## TEMPERATURE AND STRESS TRENDS

(Figure 12)

The panel temperatures and thermal stresses are related to coolant passage spacing in this figure. The temperatures influence material properties which in turn influence the thickness of material required to satisfy structural requirements. The thermal stresses add to the load stresses providing an additional impact on structural thickness requirements. Note, that as the panel temperature increases, the thermal stresses increase also so that there is a compounding of the structural weight penalties associated with increased coolant passage spacing.



# TEMPERATURE AND STRESS TRENDS

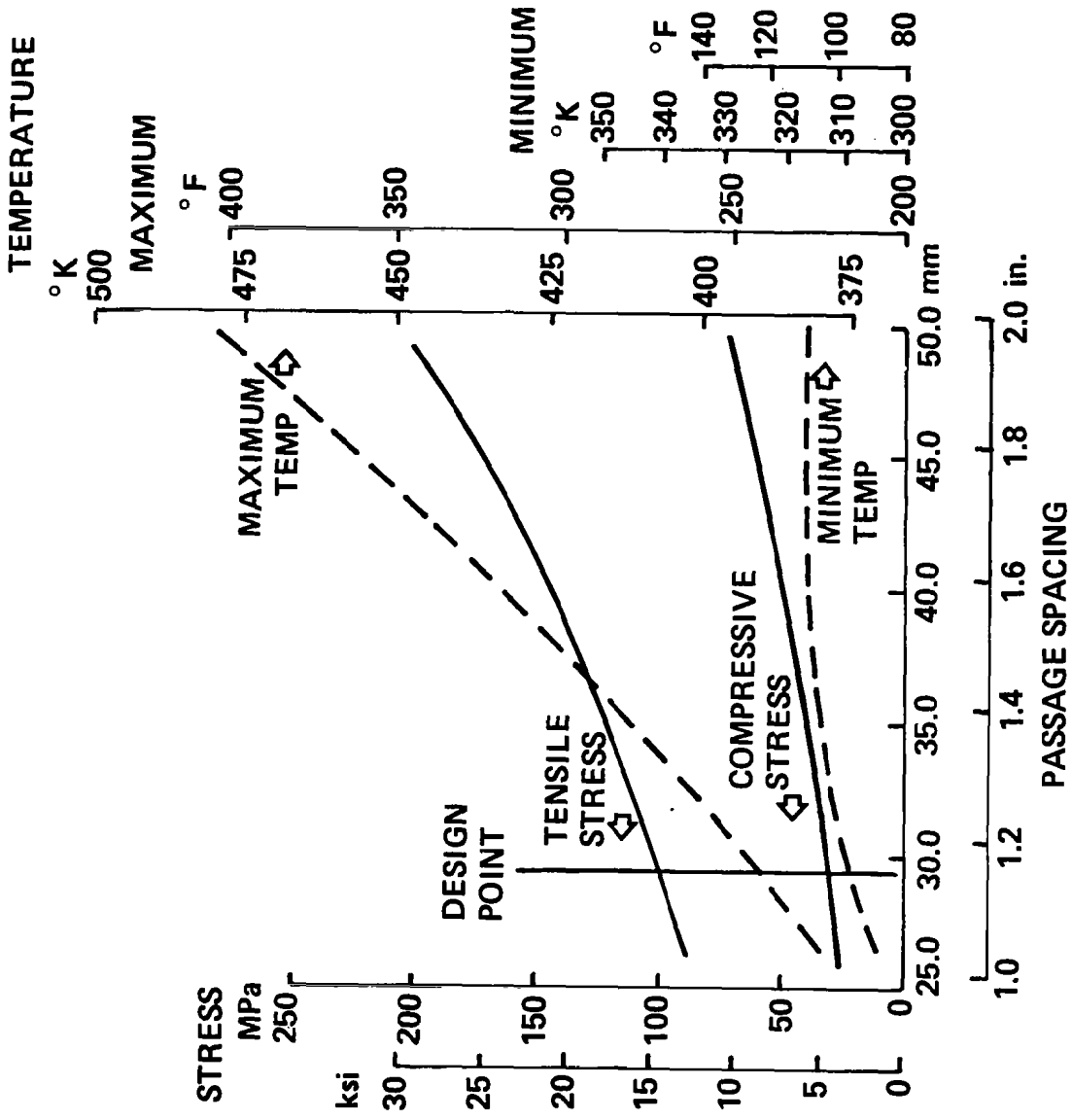


Figure 12

## MINIMUM WEIGHT IS INFLUENCED BY PRACTICAL CONSIDERATIONS

(Figure 13)

As expected, the weight of the structure increases as its operating temperature is increased. The weight of the cooling system elements decreases slightly as panel temperature is increased. The combined mass of the adhesive, coolant passage tubing, and crack stoppers shows a slight decrease with temperature increase. The net result is to decrease panel mass as temperature decreases. However, with the discrete coolant passage approach, a point is reached where it is no longer possible to incorporate stringers on the portion of the skin between coolant passages. Spacers are needed to avoid interference between the stringers and the coolant passages. The point at which spacers are needed is indicated by the step in the total and structure mass curves. The design point for the panel, therefore, was established as the configuration into which the stringers could be incorporated without the use of standoff spacers.

# MINIMUM WEIGHT IS INFLUENCED BY PRACTICAL CONSIDERATIONS

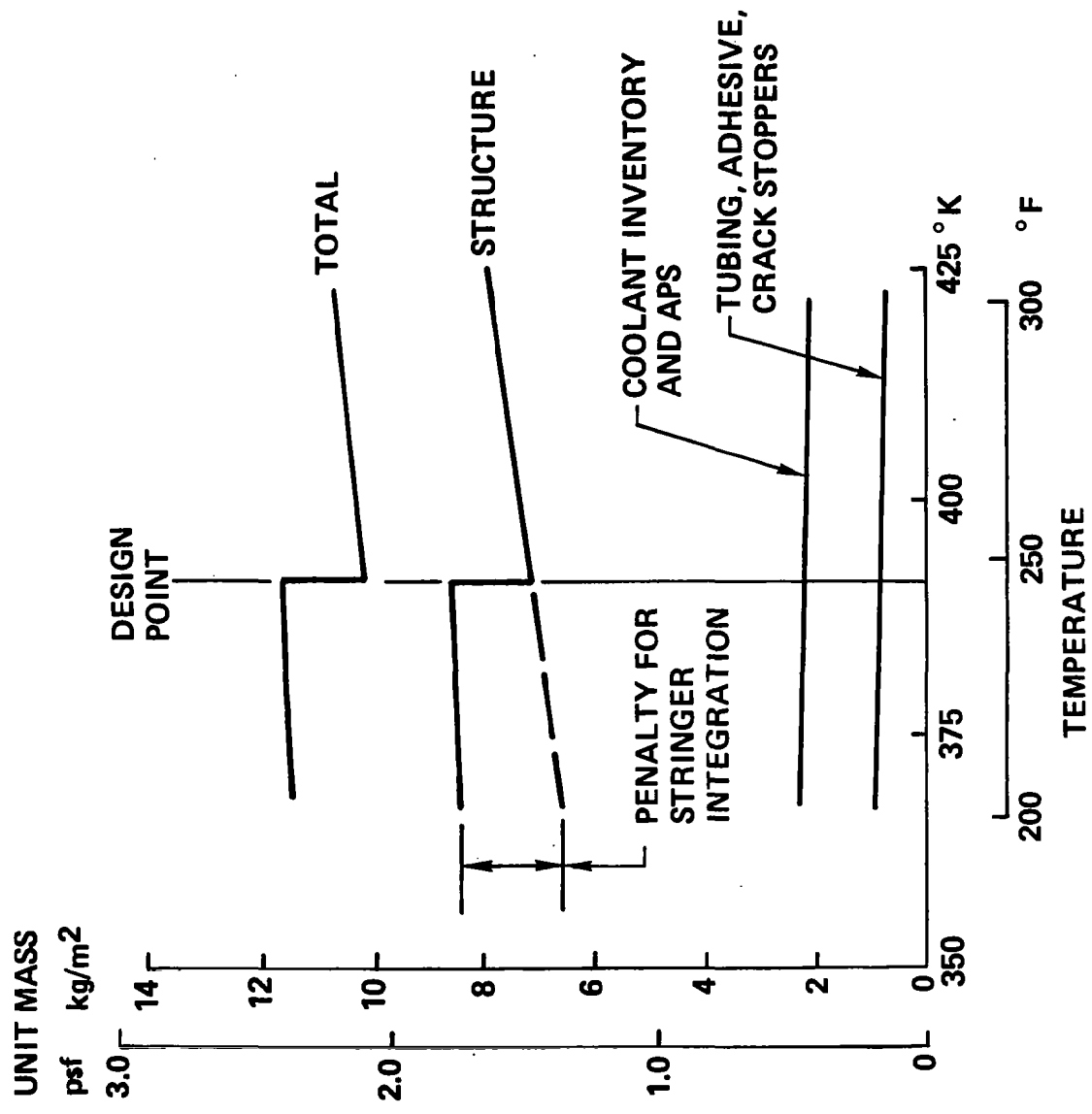


Figure 13

### TEMPERATURE AT MID LENGTH

(Figure 14)

The transverse temperature distribution (perpendicular to coolant passages) is depicted here. At the coolant passage the panel temperature is lower than it is between coolant passages. The lowest temperature is adjacent to the inner beaded skin. At the mid-length location in the panel the bulk temperature of the coolant is about  $286^{\circ}\text{K}$  ( $55^{\circ}\text{F}$ ). The large temperature difference between the coolant bulk and the coolant passage walls indicates that while most of the heat is transferred to the coolant from the flat side of the coolant passage a significant amount of heat is conducted through the beaded skin into the curved portions of the passage.

# TEMPERATURE AT MID LENGTH

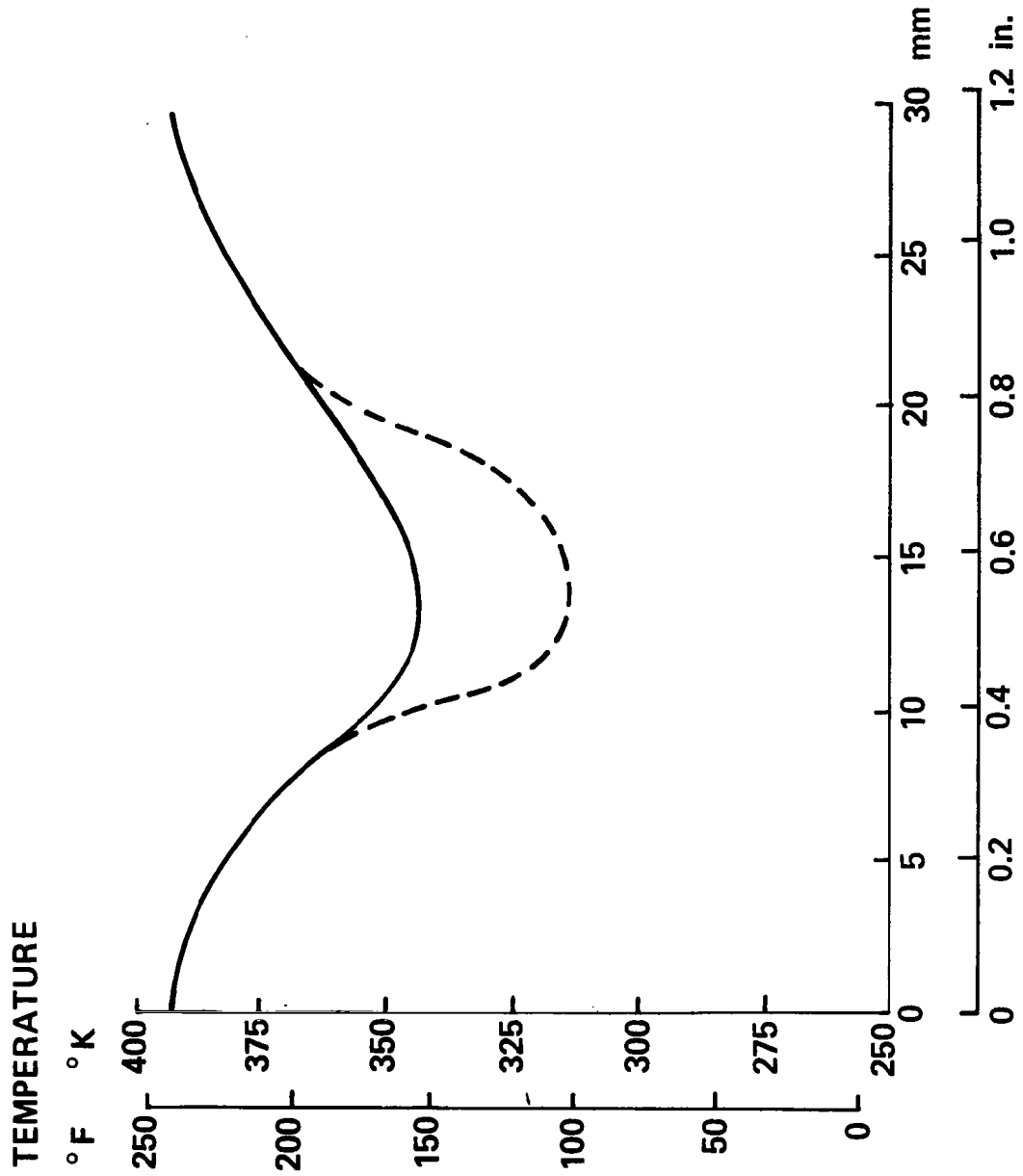


Figure 14  
LATERAL DISTANCE

## STRESS DISTRIBUTION AT MID LENGTH

(Figure 15)

Because of the temperature variation across the panel thermal stresses are generated. This plot shows the distribution of thermal stresses along the smooth outer surface of the skin, the beaded inner surface, and the stringer. Maximum tensile thermal stresses are generated in the vicinity of the cooled passage where temperatures are lowest. Compressive stresses are induced where the highest temperatures occur. It is in these regions of high compressive thermal stress that the mechanical fasteners for the stringers are installed. This tends to minimize the stress concentration effect of such fasteners. The stress induced by the alternating inplane loading is added to the thermal stress distribution when the design life is checked.

# STRESS DISTRIBUTION AT MID LENGTH

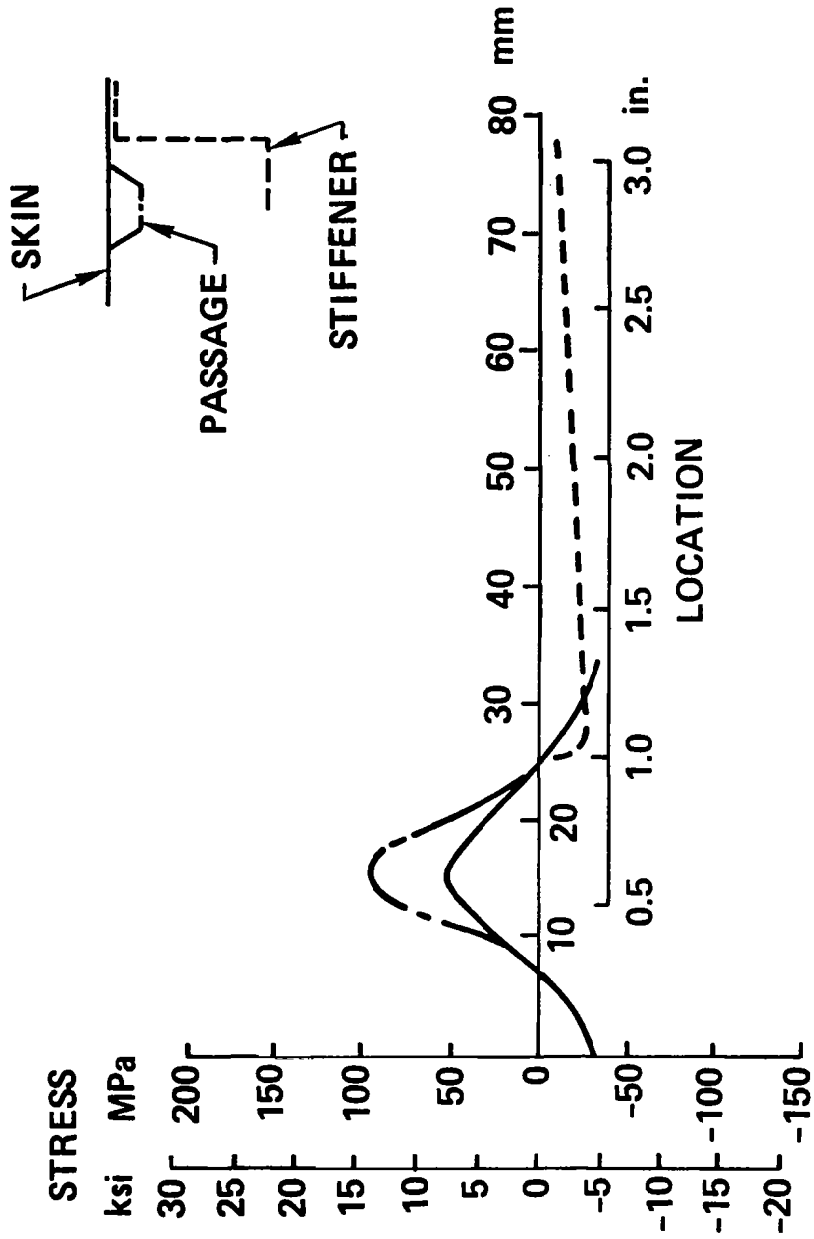


Figure 15

## PANEL FATIGUE CHARACTERISTICS

(Figure 16)

During the ground-air-ground cycle, thermal stresses grow from zero to a maximum. This is equivalent to a steady stress of half the maximum thermal stress value and an alternating stress of half the maximum value. For purposes of establishing panel thickness based on fatigue considerations, the alternating portion of the thermal stress component was added to the alternating inplane load of  $\pm 210 \text{ kN/m}^2$  ( $\pm 1200 \text{ lb/in}^2$ ). In using this applied stress, plots of steady versus alternating stresses were obtained from reference 4 for 2024-T3 alloy with appropriate stress concentration factors. The handbook data was corrected for 10,000 hours of exposure. The correction used to account for elevated temperature was an average between old ANC-5 data and the data of Dix (ref. 5). Stress concentration factors of 2.0 and 4.5 were applied to the region of the tubes and the attachment of the stringers respectively. The skin temperature was approximately  $325^\circ \text{K}$  ( $125^\circ \text{F}$ ) in the region of the tubes and  $388^\circ \text{K}$  ( $240^\circ \text{F}$ ) in the vicinity of the stringer attachment rivets. Because the compressive stresses enhance fatigue life, the equivalent thickness required to withstand the fatigue loading conditions was determined on the basis of the stresses induced in the region of tensile thermal stresses, the vicinity of the coolant passages.



# PANEL FATIGUE CHARACTERISTICS

- $\sigma = \frac{1}{2}\sigma_{th} \pm (\frac{1}{2}\sigma_{th} + \sigma_i)$
- FATIGUE ALLOWABLE REDUCED BY:
  - FACTOR FOR 10,000 HOURS OF EXPOSURE
  - TEMPERATURE
  - STRESS CONCENTRATION OF 2.0 AND 4.5
- DESIGN LIFE OF 20,000 CYCLES (5000 x 4.0)
- EQUIVALENT THICKNESS REQUIRED = 0.51 mm (0.11 in.)

## PANEL STABILITY CHARACTERISTICS

(Figure 17)

Having established the equivalent skin thickness to meet the life requirement, the material is proportioned to maximize panel stability. Early studies had indicated that stringer depth and thickness of about 3.8 mm (1.50 in) and 0.127 mm (0.050 in) were near optimum. The stringer pitch was dictated by the coolant passage spacing. Fabrication and efficiency considerations dictated Zee stringers. The skin thickness was dictated by convenient sheet thicknesses and a desire to apportion the equivalent thickness on an approximate 50/50 basis with the stringers. The stringer sizing was accomplished using a computer optimization code which accounted for axial loading and normal pressure loading. The computer code generated nonbuckling and buckling designs, the results of which are plotted. The thermal moment was introduced as an additional increment of normal pressure loading.

As can be seen from the figure, the particular proportions selected would permit an axial loading of approximately 470 kN/m (2700 lb/in) to be carried without inducing buckling while the axial load carried as the panel buckles would be approximately 580 kN/m (3300 lb/in). The analyses assumed a material temperature of 408°K (250°F). The panel is able to carry more than twice the design inplane loading without buckling.

# PANEL STABILITY CHARACTERISTICS

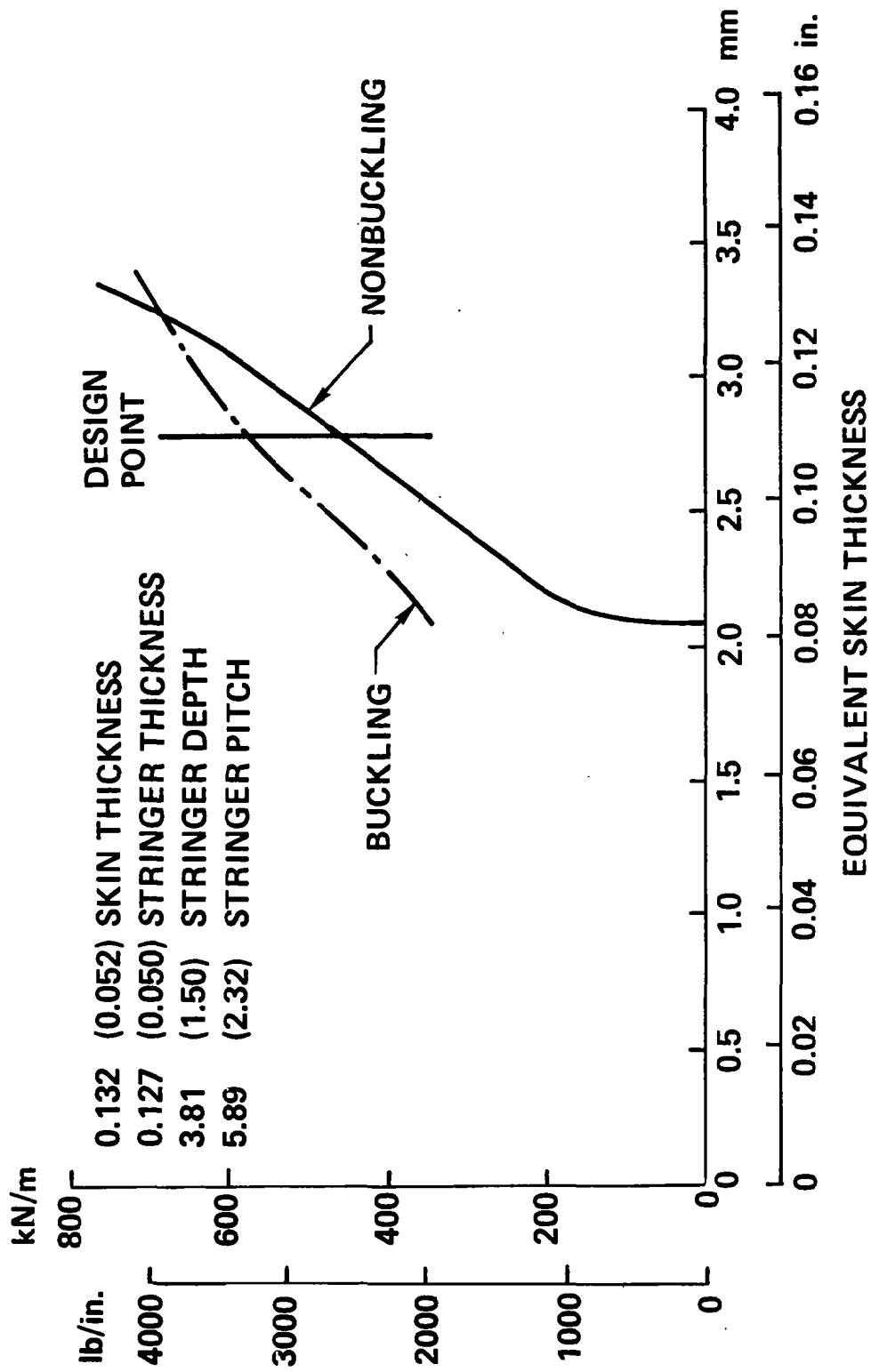


Figure 17

## EXPERIMENTAL STUDIES

(Figure 18)

The initial plan envisioned validation of panel design details via a series of fatigue tests conducted at the Langley Research Center. During the fabrication of these specimens, areas in need of process refinement were identified. The NASA tests identified some areas of deficiency. Therefore, the experimental study effort was expanded to include five additional types of specimens, four of which involved aspects of adhesive utilization.

# EXPERIMENTAL STUDIES

<u>SPECIMEN TYPE</u>	<u>PURPOSE</u>
● NASA FATIGUE (6)	— VALIDATE PANEL DETAILS
● MANIFOLD END PLUG (13)	— SELECT ADHESIVE
● COOLANT PASSAGE PLUG (10)	— SELECT POTTING COMPOUND
● PRESSURE PANEL (4)	— VALIDATE PRESSURE INTEGRITY
● EDGE ATTACHMENT (15)	— VALIDATE DESIGN CHANGE
● MANIFOLD REPAIR (1)	— VALIDATE REPAIR TECHNIQUE

### FATIGUE AND PRESSURE TEST SPECIMENS WERE CUT FROM A COOLED SKIN PANEL

(Figure 19)

In order to establish preliminary manufacturing procedures it was decided to fabricate a 0.61 x 1.22 m (24 x 48 in) cooled skin panel from which test specimens could be cut. The cutting plan is shown here. Leakage observed during the fatigue tests was investigated with the pressure test specimens. The fabrication procedures were those intended for use on the final test panel. Some difficulties were encountered and procedures were modified accordingly. Of particular importance were refinements in the methods for applying the silver filled Eccobond 58C adhesive.

# FATIGUE AND PRESSURE TEST SPECIMENS WERE CUT FROM A COOLED SKIN PANEL

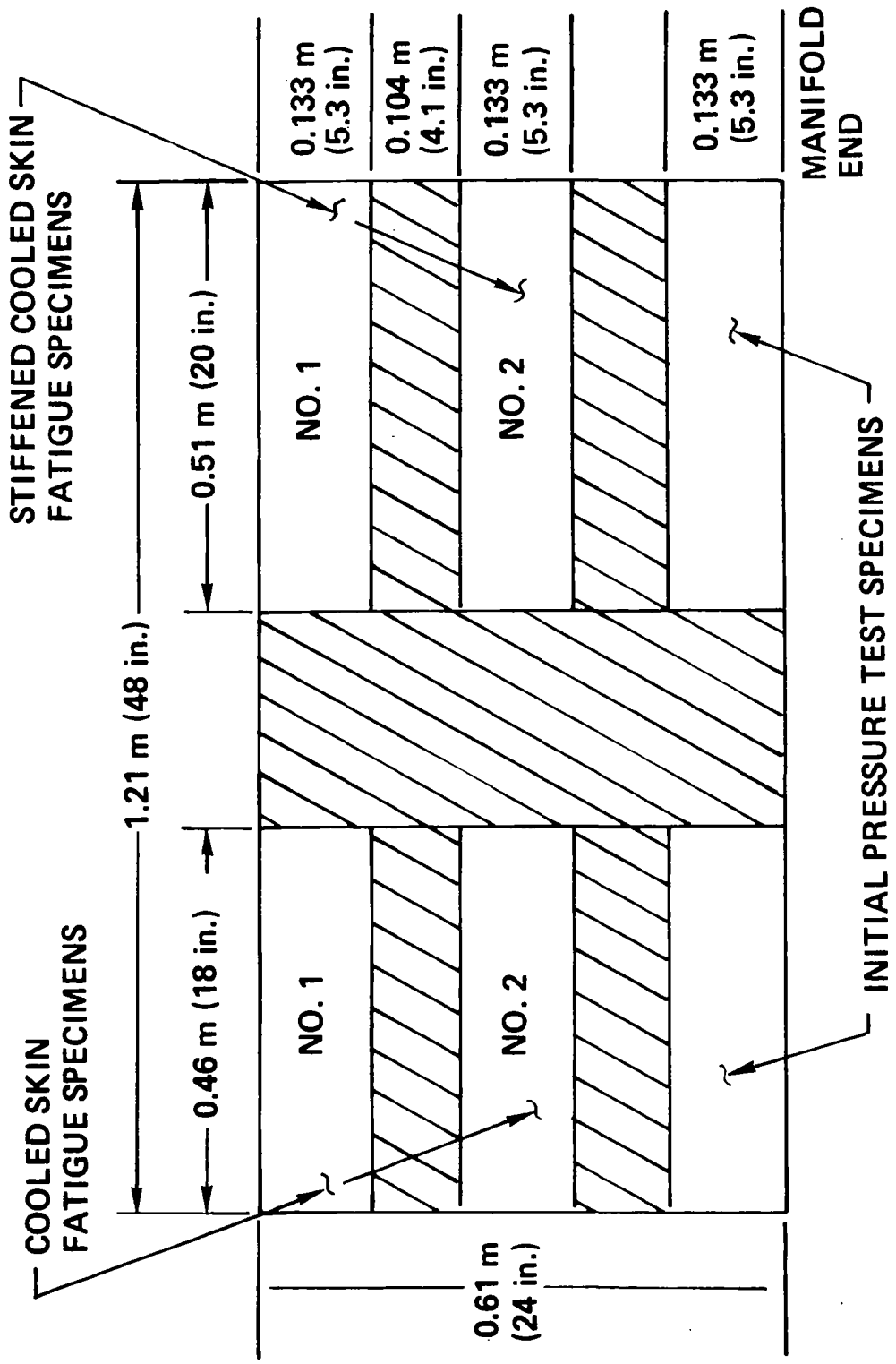


Figure 19

## UNSTIFFENED FATIGUE SPECIMENS

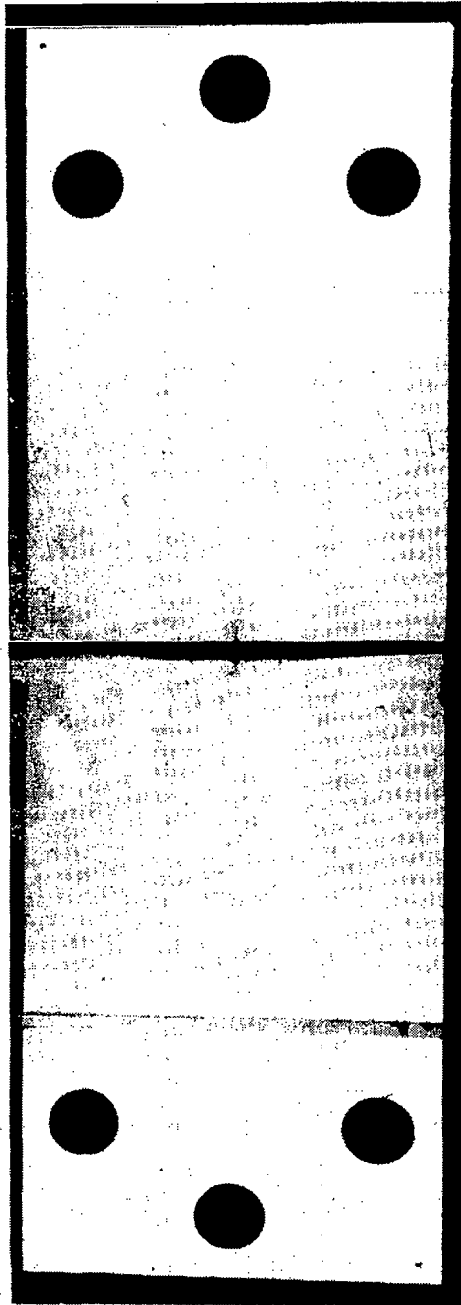
(Figure 20)

Two types of unstiffened fatigue specimens were fabricated for evaluation at Langley Research Center. The first type (upper photo) consisted of two flat sheets bonded together by alternating stripes of Epon 951 and Eccobond 58C. After surviving 20,000 cycles at the desired load level, notches were machined into the skin and allowed to propagate until failure. When a through notch was used crack propagation proceeded in much the same manner as would be expected of aluminum alloy sheet having the total thickness of the bonded skin. When a surface notch was introduced the bond line delayed the progression of the crack from the notched skin to the other skin layer.

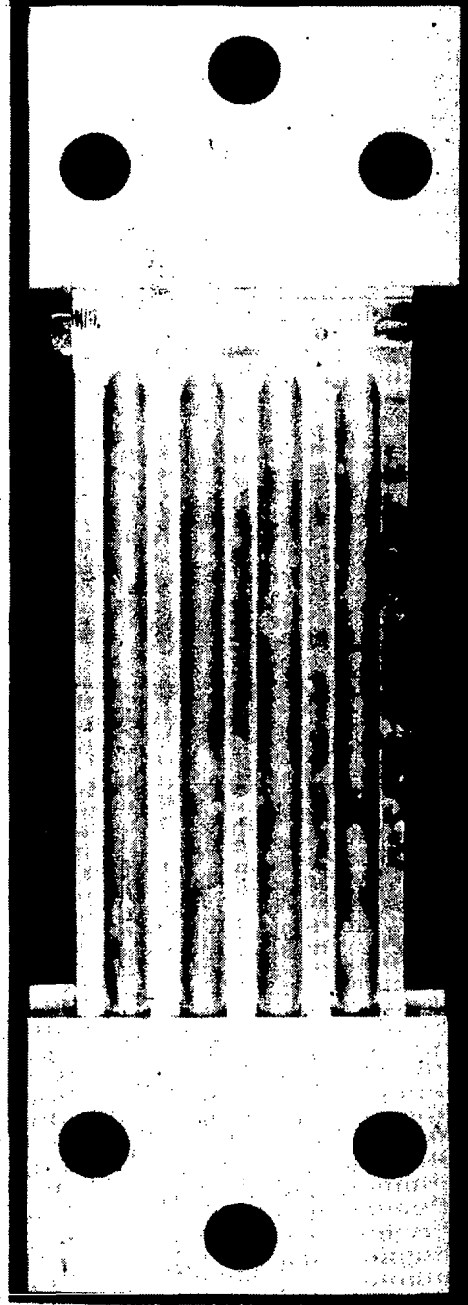
The lower photo illustrates the second type of unstiffened fatigue specimen which incorporated the transition between the manifold region and the inboard portion of the skin panel/tube assembly. Small squares of teflon replaced some of the adhesive film in the sloping portion of the transition. After sustaining 20,000 cycles at the design load, notches were introduced and the panel and the specimens were cycled to failure. The crack stoppers at the edges of the coolant passages appeared to delay the progress of crack growth slightly. Some leakage of the pressurized fluid within the panel was noted prior to rupture of the coolant passage tubing.



**UNSTIFFENED FATIGUE SPECIMENS**



SKIN



COOLANT PASSAGE/RAMP

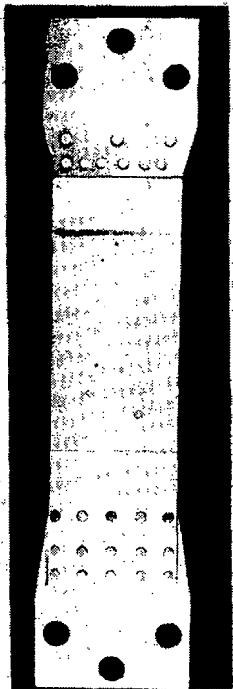
Figure 20

## STIFFENED FATIGUE SPECIMEN

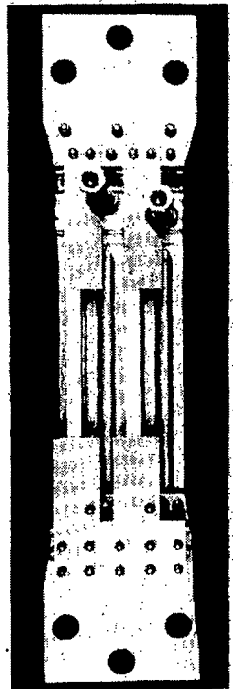
(Figure 21)

The major features of the cooled panel design were incorporated in these specimens. Initial loadings indicated significant deformations at the single shear spliced joint. A double shear joint was introduced and fatigue testing was continued. Leakage of the pressurized oil within the panel was noted early in the testing. This necessitated deletion of the pressurization aspect of the fatigue tests. Both specimens failed from cracks that started at the rivets. One sustained 17,900 cycles while the other sustained 19,500 cycles. While not quite as long as the 20,000 cycle target, the results were considered adequate for verifying the design features.

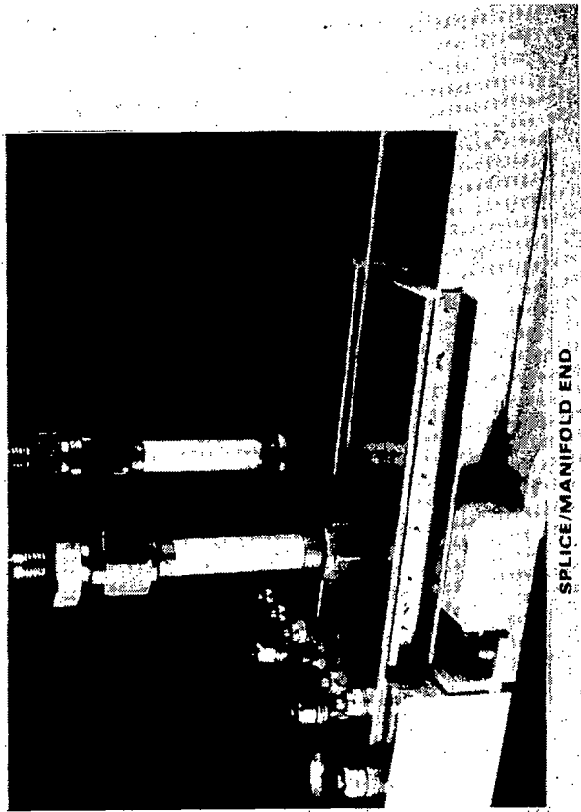
**STIFFENED FATIGUE SPECIMEN**



**TOP VIEW**



**BOTTOM VIEW**



**SPICE/MANIFOLD END**

**Figure 21**

## EXPERIMENTAL RESULTS

(Figure 22)

Based on the various experimental evaluations that were conducted, details of the cool panel design and the associated fabrication procedures were verified. The experimental effort required to validate manufacturing procedures was significantly greater than anticipated. As is often the case, the design concept was relatively straightforward but its successful implementation required great attention to details. The manufacturing procedures which required refinement were all associated with the use of adhesives. While it was not necessary to develop any new materials, it was necessary to compare alternate approaches before selections could be made for specific functions. The experimental results did verify that adhesive bonding could be used even when the most critical bond line thicknesses were small compared to manufacturing tolerances associated with machining and sheet metal forming.

## EXPERIMENTAL RESULTS

- NASA FATIGUE
  - BONDED SKIN
    - SIMILAR TO SINGLE THICKNESS
  - TRANSITION
    - ADEQUATE FATIGUE LIFE, LEAKAGE
  - STIFFENED
    - INADEQUATE SPLICE DESIGN, LEAKAGE
- MANIFOLD END PLUG
  - ALUMINA FILLED EPON 828 SELECTED
- COOLANT PASSAGE PLUG
  - ALUMINA FILLED EPON 828 SELECTED
- PRESSURE PANEL
  - TIGHTER TOLERANCES NEEDED ON TUBING,  
IMPROVED MANUFACTURING TECHNIQUES  
DEVELOPED
- EDGE ATTACHMENT
  - CHERRYBUCK RIVETS USED IN DOUBLE SHEAR
- MANIFOLD REPAIR
  - BLIND RIVETS SEALED WITH SCOTCH WELD 1838

## TEST PANEL - TOP VIEW

(Figure 23)

This figure shows the test panel and one of the two adapters which will be used for applying inplane loads. The panel configuration is no different than would be expected for a conventional skin/stringer/frame structural panel. Close examination of the actual panel with properly reflected light shows a slight undulating pattern related to the location of coolant passages. Each load adapter will introduce the inplane loading at 21 discrete locations through straps which accommodate thermal expansions. The three sets of plates at the ends of the frames will attach to the NASA test fixturing to simulate continuous frames.

**TEST PANEL - TOP VIEW**

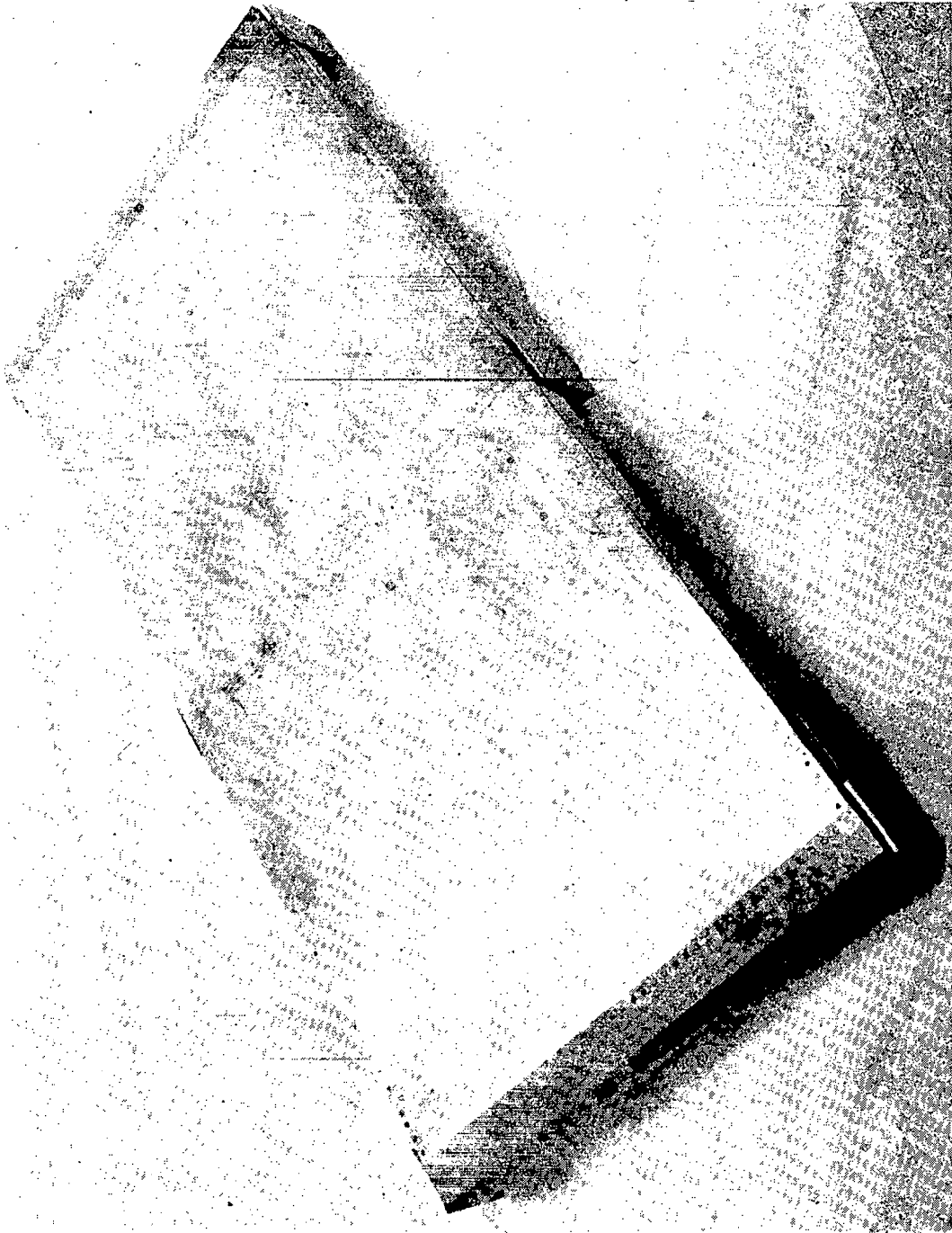


Figure 23

**COOLED SKIN – BOTTOM VIEW**

(Figure 24)

The transition of the coolant circuitry from the end manifolds to the coolant passages is depicted here. Parallel adjacent plenums are machined in the manifold blocks perpendicular to the coolant passage length. The manifold block tapers at the inboard transition to the bonded skin. The outer edge of the manifold block provides for the splice which would join the cooled panels perpendicular to the primary load direction.



COOLED SKIN - BOTTOM VIEW

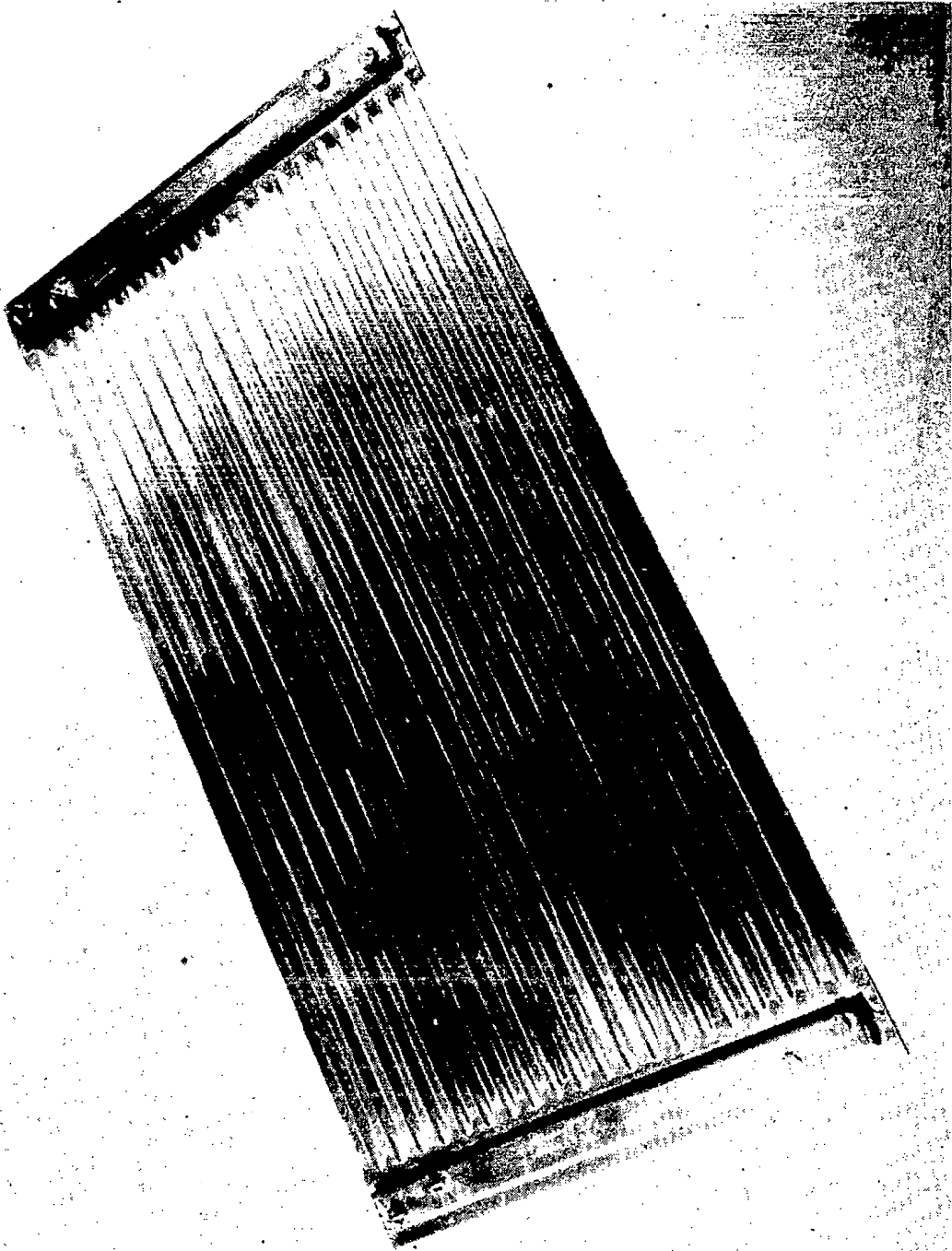


Figure 24

## TEST PANEL – BOTTOM VIEW

(Figure 25)

When the substructure is added to the cooled skin panel it is difficult to identify the coolant passages and the manifold installation. Dominant features are the stringers and the large end attachments for the load adapters. The transitions from the load adapter to the cooled structural panel are designed conservatively so that the margins of safety are lower in the panel proper than in the test fixturing.

TEST PANEL - BOTTOM VIEW

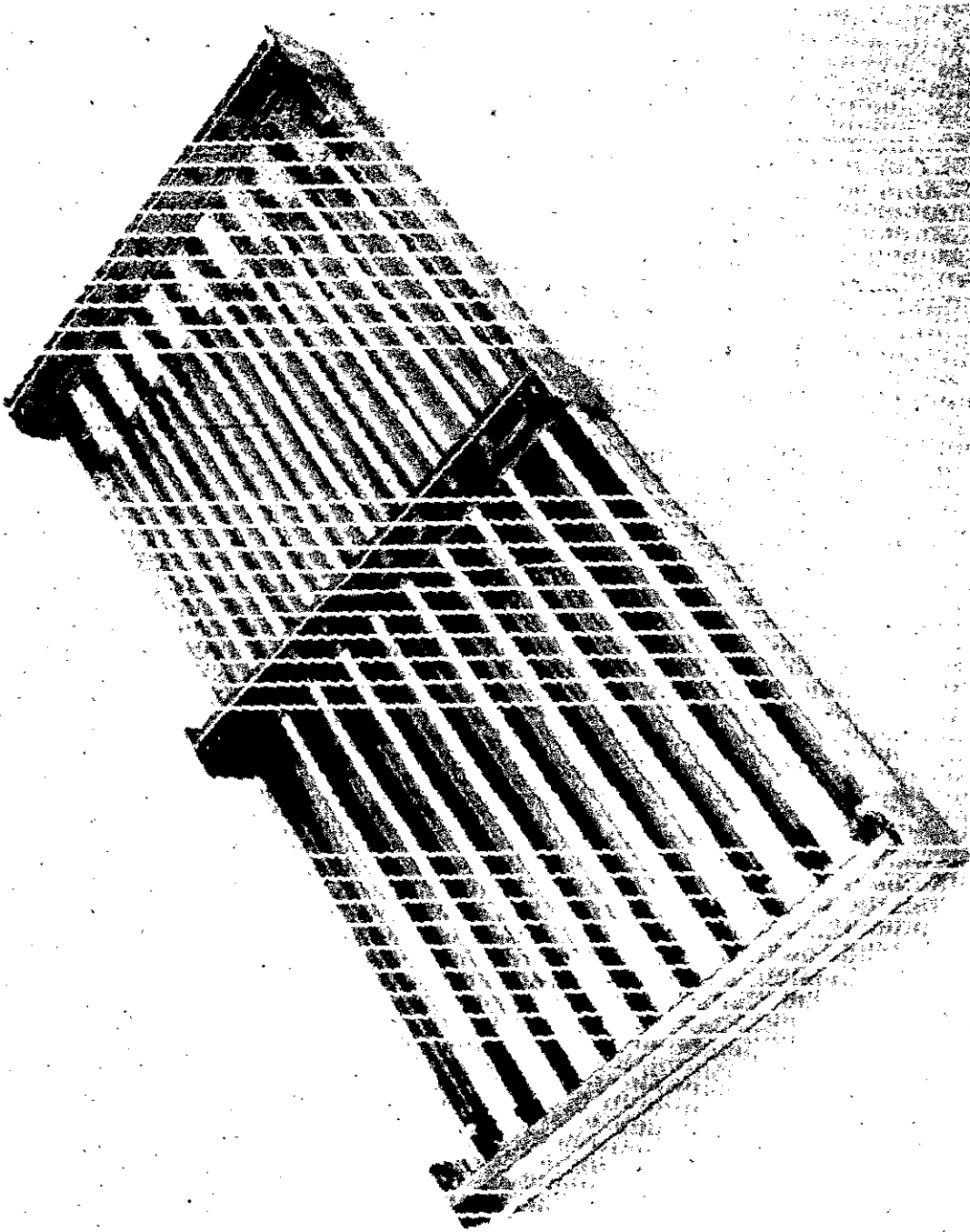


Figure 25

## CENTER FRAME DETAILS

(Figure 26)

The details of integrating the stringers and frames with the cooled skin are illustrated here. The stringers are riveted directly to the cooled skin in the region between coolant passages. The stringers are attached to the frames by right angle clips and a right angle cap. The height of the coolant passages necessitates the use of small spacers at the skin to frame attachment. All of the riveting in this region is relatively accessible.

**CENTER FRAME DETAILS**

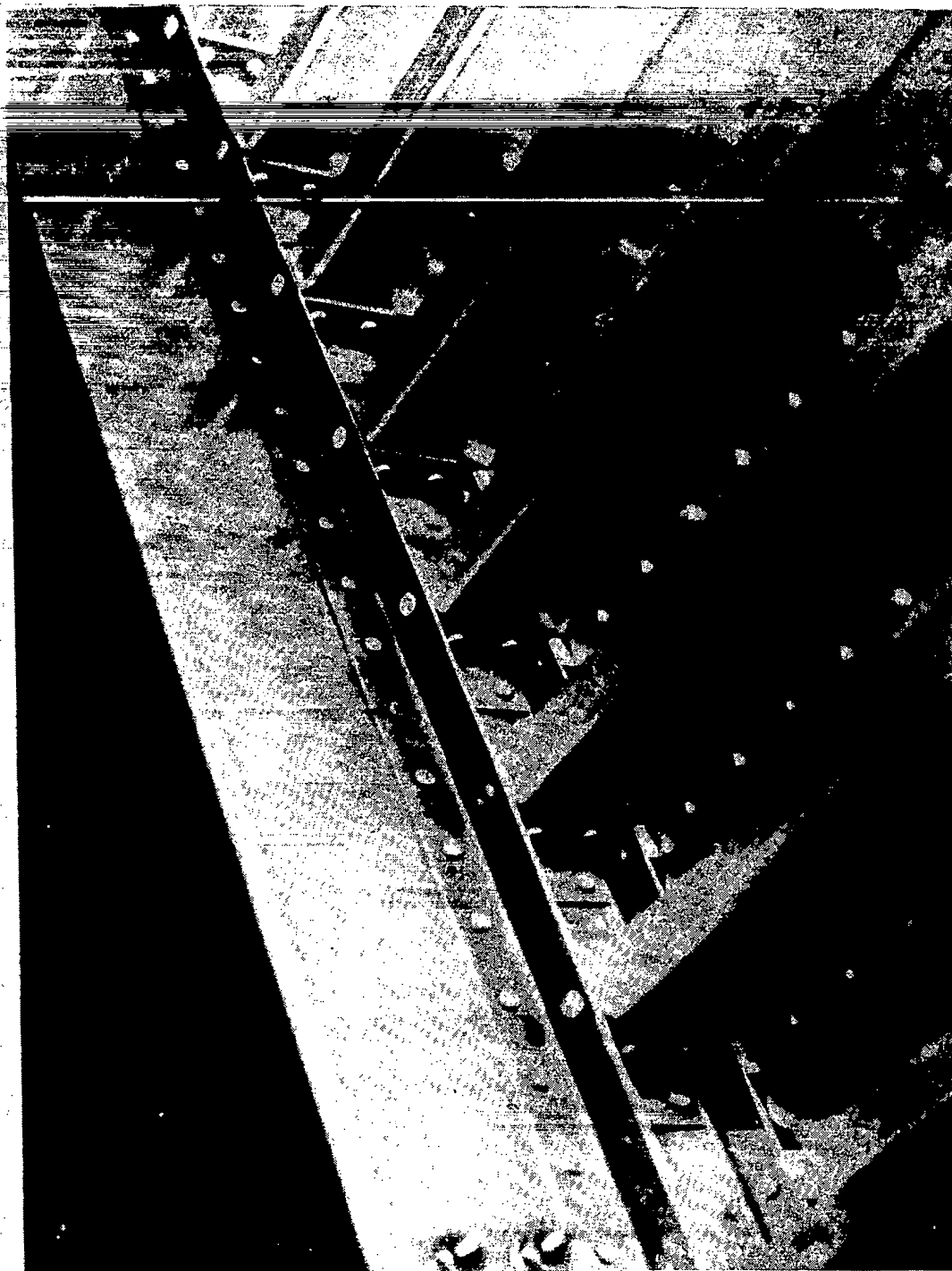


Figure 26

## END FRAME AND STRINGER DETAILS

(Figure 27)

Installation of the details at the end frames is somewhat more complex than at the center frame. Because of the coolant manifold, it is necessary to notch each stringer and to reinforce the inner flange with a formed channel. To properly introduce the inplane load at the neutral axis of the panel, extruded T-sections were attached to the stringers. The titanium straps from the load adapter arrangement attach to the flanges of these T's as well as the double shear splice joint at the outer edge of the panel.

**END FRAME AND STRINGER DETAILS**

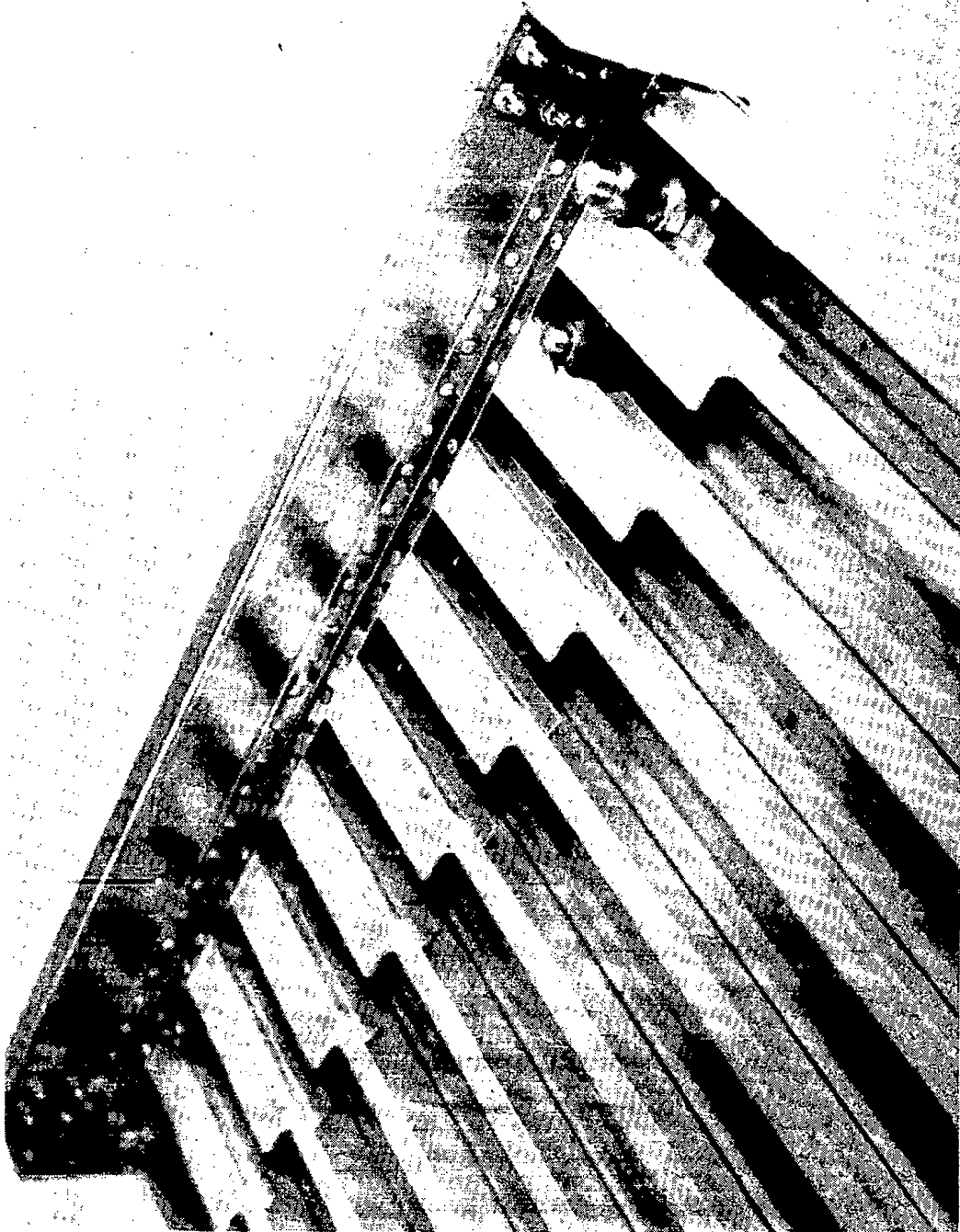


Figure 27

## SPLICE AND END FRAME DETAILS

(Figure 28)

In an actual application it would be necessary to splice the cooled skins and perhaps the stringers also. The skin splice transmits about 85% of the inplane loading. This splice is made to an extruded aluminum T that forms the outer cap of the frame and a titanium splice plate along the external surface. Titanium was necessary because this external splice plate cannot be cooled down to temperatures where aluminum alloys could be considered. The extruded T's at the inner stringer flange simulate splice plates for the stringers.



**SPLICE AND END FRAME DETAILS**

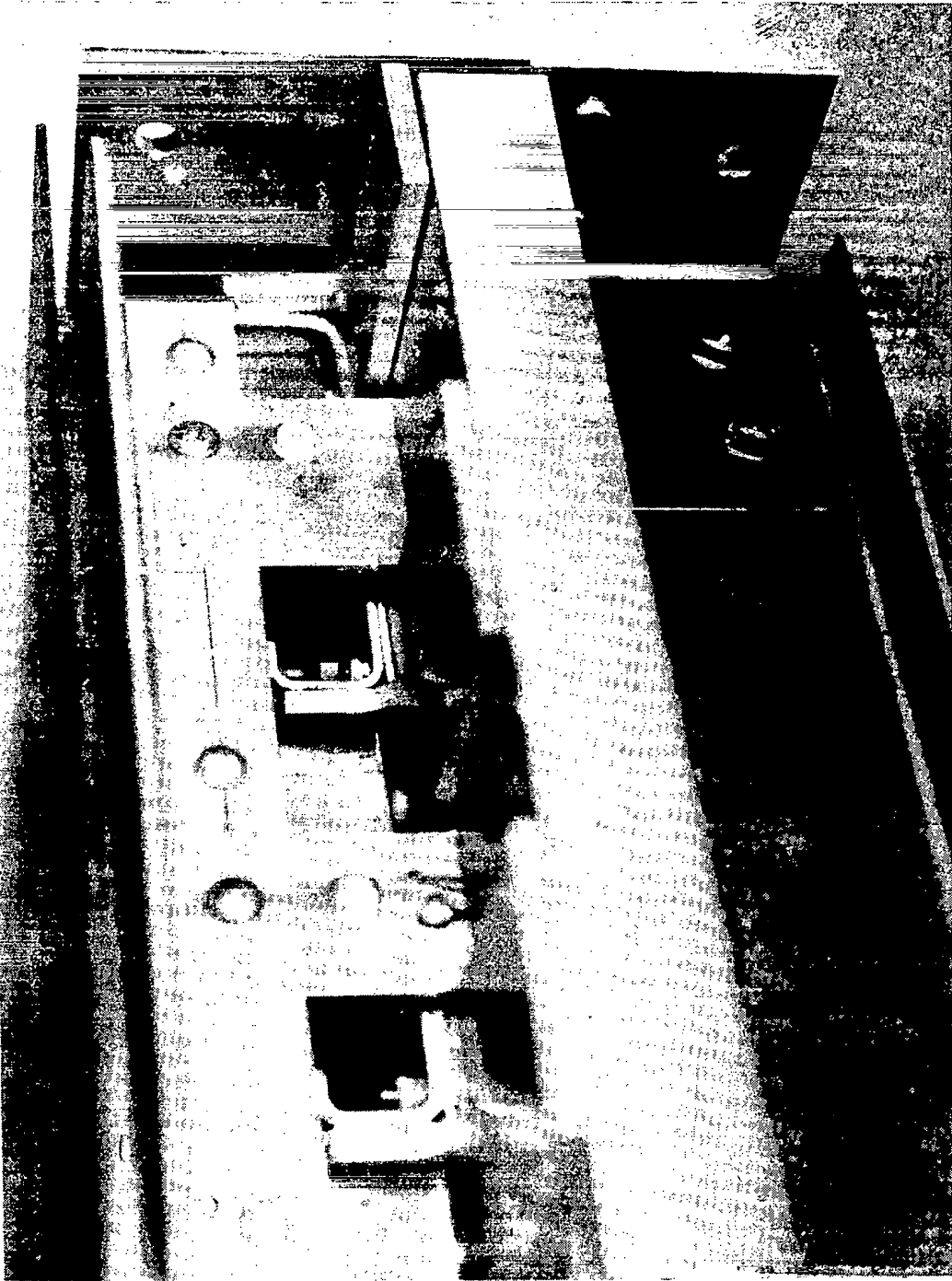


Figure 28

## APPLICATION OF SILVER FILLED EPOXY

(Figure 29)

One of the most difficult fabrication operations was the application of the silver filled epoxy adhesive. This material was used between the coolant passages and the inner beaded skin, and as stripes for bonding the outer skin. The silver filled epoxy was troweled into the beads of the panel used for the fatigue specimens. Several types of spatula like devices and numerous technique variations were investigated. All were time consuming. When the final test panel was to be fabricated the need for improved techniques was recognized. A caulking gun approach seemed highly desirable. The "as received" consistency was thinned with MEK and toluene as diluents. For the relatively large beads of adhesive that were to be applied in this application thinning with between 2 and 3% of diluent was adequate for obtaining good flow of the adhesive at modest pressure. Excess adhesive was applied, the tubes were installed, and the system was debulked in two steps. Most of the excessive silver filled adhesive, which extruded from around the coolant passage tubing during the first debulking cycle, was removed prior to the second cycle. The second cycle was required because the squeeze out from the first cycle precluded obtaining a flat surface across the entire panel as the passages and skin was squeezed against the heavy caul plate.

The stripes of Eccobond 58C adhesive used in bonding the smooth outer skin to the inner subassembly were applied with a caulking gun technique as well. The small quantity of adhesive needed for each stripe required that the silver filled epoxy be thinned with about 4 to 5% diluent.

Toluene was chosen as the more desirable diluent. A minimum of 1 hour exposure in air was used before parts were mated to allow most of the diluent to evaporate.

**APPLICATION OF SILVER FILLED EPOXY**

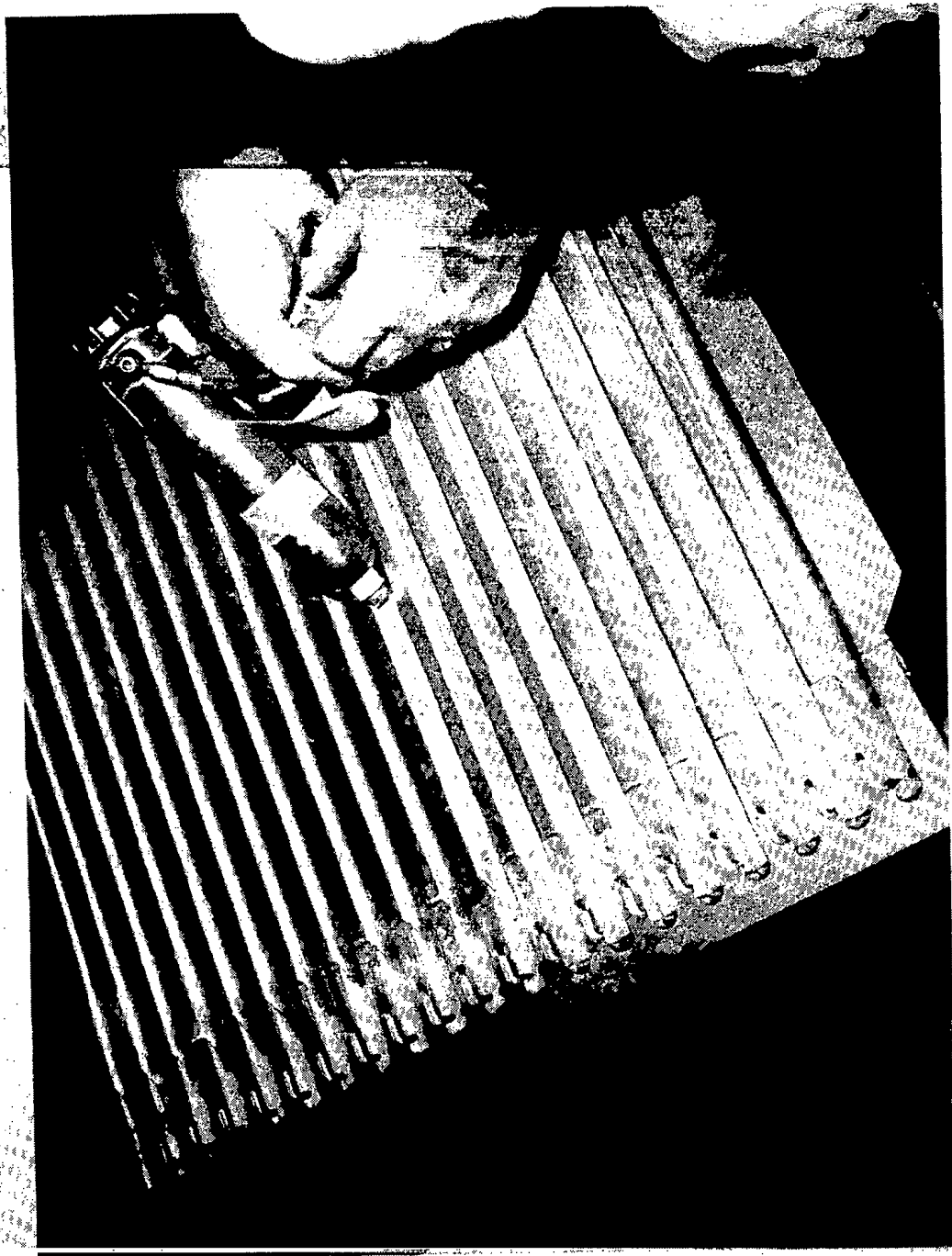


Figure 29

## HOLOGRAMS OF PANEL SUBASSEMBLY, NO OUTER SKIN

(Figure 30)

A considerable effort was devoted to investigating nondestructive inspection techniques for use with bonded actively cooled panels. Radiography was used to identify the uniformity of those adhesive joints made with the silver filled epoxy. Tests with low pressure gas were used to identify leaks at various stages of the assembly fabrication. Holography was used to investigate the uniformity of bonding of the coolant passage tubing into the manifold/inner skin subassembly and to ascertain whether any of the coolant passages became plugged during bonding operations.

The holograms shown in this figure indicate the degree of uniformity achieved in the bonding operation. Careful examination of the holograms in the vicinity of the ends of the coolant passages indicates slight nonuniformity in the depth of end plug potting and apparent blockage in coolant passages.

Note in the lower photos the difference between the general pattern and those of the ninth tube from the left and the twelfth tube from the right. The former indicates an anomaly although the tube is pressurized. The latter indicates that the tube is blocked at both ends and is not pressurized.

**HOLOGRAMS OF PANEL SUBASSEMBLY, NO OUTER SKIN**

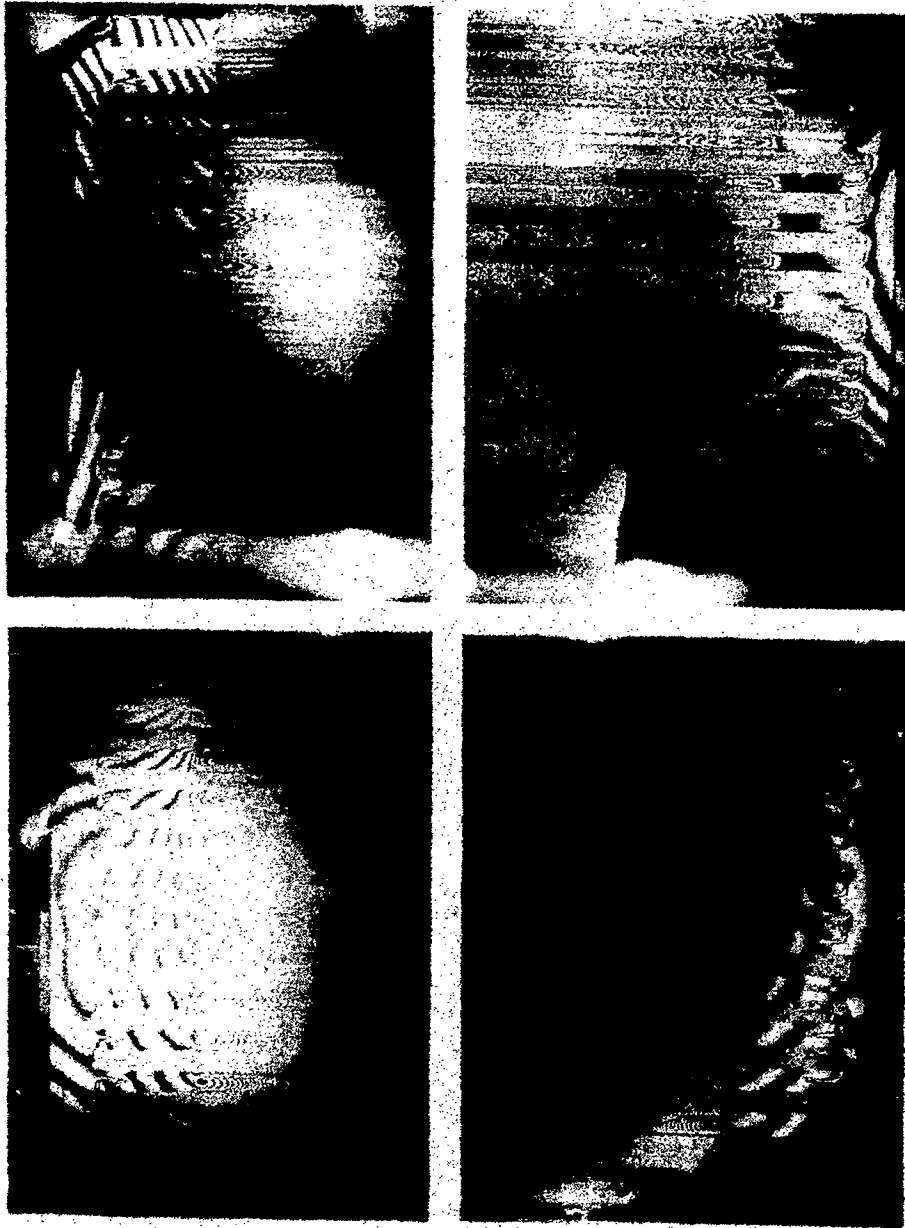


Figure 30

## INFRARED SCAN RESULTS AFTER REWORK

(Figure 31)

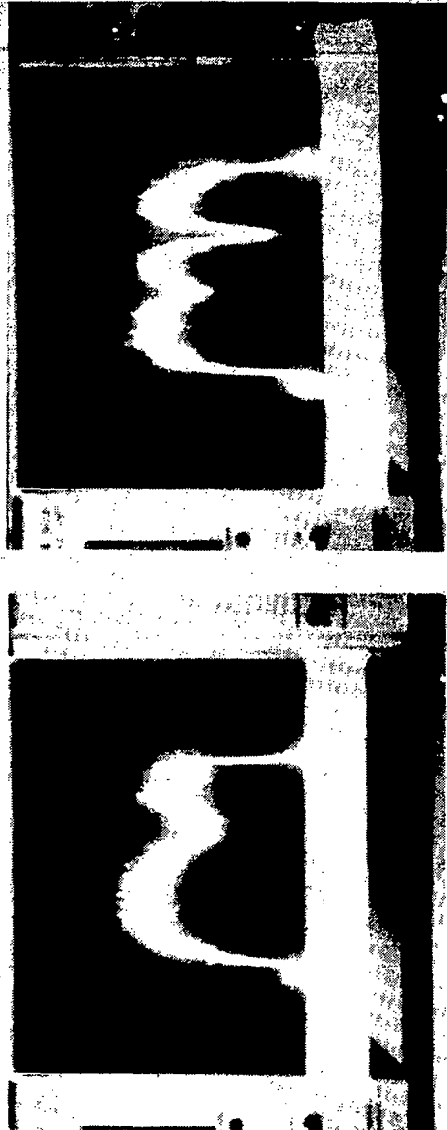
Because of tolerances it was necessary to use thicker bondlines than anticipated between the coolant passage tubing and the manifolds. Despite the fact that the Epon 951 adhesive has low flow in thin thicknesses, the use of multiple layers increased the amount of flow. The holes between the manifolds and the coolant passages became plugged with excess adhesive. This condition was observed visually on some of the end holes, defined further through boroscopic inspection, and the severity was established by the nonuniformity of infrared scans across the panel.

After rework to open the holes between the manifold and the coolant passage tubing the infrared scans were repeated with the results shown here. The temperature of the water flowing through the panel was varied so that the scans could be made under transient conditions to maximize temperature differences. As indicated by these scans the coolant flow through the parallel passages was relatively uniform. Only one passage in each circuit lags the others to any significant degree. The flow through the end edge tubes appeared to be slightly less than average. The majority of the coolant passages did have uniform flow as evidenced by the general uniformity of temperature across the panel. Careful examination of the scans revealed the higher temperature between coolant passages and the lower temperature at the coolant passage. On casual observation these differences in temperature create the appearance of a rather wide scatter band.

**INFRARED SCAN RESULTS AFTER REWORK**



**FLOW TO INBOARD MANIFOLD**



**FLOW TO OUTBOARD MANIFOLD**

**SECOND CIRCUIT**

**FIRST CIRCUIT**

Figure 31

## CONCLUDING REMARKS

(Figure 32)

Until the test panel is evaluated experimentally, it seems premature to draw conclusions. The work performed to optimize the full sized panel and to fabricate the test panel led to some observations that are presented as concluding remarks. Special attention is called to the accomplishment of the tubing fabricator who produced the unusual coolant passage shape to very stringent tolerances. Precision Tube was the only supplier willing to guarantee delivery out of twenty suppliers from whom quotes were requested.



## **CONCLUDING REMARKS**

- **STRUCTURAL CONSIDERATIONS ARE DOMINANT IN THE DESIGN OF ACTIVELY COOLED STRUCTURAL PANELS OF MINIMUM MASS**
- **WHEN HEAT FLUXES ARE IMPOSED DIRECTLY ONTO AN ACTIVELY COOLED STRUCTURAL PANEL THE USE OF ADHESIVE BONDING PERMITS THE USE OF OPTIMUM STRUCTURAL MATERIALS**
- **VARIOUS DIFFICULTIES ASSOCIATED WITH THE ACCOMMODATION OF MACHINING AND FORMED SHEET METAL TOLERANCES WITH THIN BOND LINES WERE RESOLVED**
- **NONDESTRUCTIVE INSPECTION TECHNIQUES WERE ADAPTED TO THE UNIQUE REQUIREMENTS OF AN ACTIVELY COOLED STRUCTURAL PANEL**

## REFERENCES

1. Nowak, R.J. and Kelly, H.N., "Actively Cooled Airframe Structures for High-Speed Flight," 17th Structures, Structural Dynamics, and Materials Conference Proceedings, May 1976, p. 209-217.
2. Helenbrook, R.G. and Anthony, F.M., "Design of a Convective Cooling System for a Mach 6 Hypersonic Transport Airframe," NASA CR-1918, December 1971.
3. Anthony, F.M., Dukes, W.H. and Helenbrook, R.G., "Internal Convective Cooling Systems for Hypersonic Aircraft," NASA CR-2480, February 1975.
4. Department of Defense, "Metallic Materials and Elements for Aerospace Vehicle Structures," MIL-HDBK-5A, Revised 5 January 1970.
5. Kroll, W.D., "Aerodynamic Heating and Fatigue," NASA Memo 6-4-59W, June 1959.